Carbohydrate Polymers 175 (2017) 178–191

Contents lists available at ScienceDirect

Carbohydrate Polymers

journal homepage: www.elsevier.com/locate/carbpol

Tilia tomentosa pectins exhibit dual mode of action on phagocytes as β-glucuronic acid monomers are abundant in their rhamnogalacturonans I

Yordan N. Georgiev[a,b], Berit S. Paulsen[c], Hiroaki Kiyohara[d], Milan Ciz[e], Manol H. Ognyanov[a,b], Ondrej Vasicek[e,i], Frode Rise[f], Petko N. Denev[a,b], Antonin Lojek[e], Tsvetelina G. Batsalova[g], Balik M. Dzhambazov[g], Haruki Yamada[d], Reidar Lund[f], Hilde Barsett[c], Albert I. Krastanov[h], Irina Z. Yanakieva[a,b], Maria G. Kratchanova[a,b,*]

[a] *Laboratory of Biologically Active Substances, Institute of Organic Chemistry with Centre of Phytochemistry, Bulgarian Academy of Sciences, 139 Ruski Blvd., BG-4000, Plovdiv, Bulgaria*
[b] *Innovative-Technological Center Ltd., 20 Dr. G. M. Dimitrov Str., BG-4000, Plovdiv, Bulgaria*
[c] *Department of Pharmaceutical Chemistry, School of Pharmacy, University of Oslo, P.O. Box 1068 Blindern, NO-0316, Oslo, Norway*
[d] *Department of Drug Discovery Science, Kitasato Institute for Life Sciences, Kitasato University, 5-9-1 Shirokane, Minato-ku, JP-108-8641, Tokyo, Japan*
[e] *Department of Free Radical Pathophysiology, Institute of Biophysics, Czech Academy of Sciences, 135 Kralovopolska, CZ-612 65, Brno, Czech Republic*
[f] *Department of Chemistry, University of Oslo, P.O. Box 1033 Blindern, NO-0315, Oslo, Norway*
[g] *Department of Developmental Biology, Plovdiv University Paisii Hilendarski, 24 Tsar Assen Str., BG-4000, Plovdiv, Bulgaria*
[h] *Department of Biotechnology, University of Food Technologies, 26 Maritza Blvd., BG-4002, Plovdiv, Bulgaria*
[i] *International Clinical Research Center – Center of Biomolecular and Cellular Engineering, St. Anne's University Hospital Brno, 53 Pekarska, CZ-656 91, Brno, Czech Republic*

ARTICLE INFO

Article history:
Received 1 June 2017
Received in revised form 21 July 2017
Accepted 24 July 2017
Available online 25 July 2017

Keywords:
Tilia flowers
Pectin
Immunomodulating polysaccharides
Anti-inflammatory activity
Neutrophils
Peyer's patches

ABSTRACT

Silver linden flowers contain different pectins (PSI-PSIII) with immunomodulating properties. PSI is a low-esterified pectic polysaccharide with predominant homogalacturonan region, followed by rhamnogalacturonan I (RGI) with arabinogalactan II and RGII (traces) domains. PSII and PSIII are unusual glucuronidated RGI polymers. PSIII is a unique high molecular weight RGI, having almost completely O-3 glucuronidated GalA units with >30% O-3 acetylation at the Rha units. Linden pectins induced reactive oxygen species (ROS) and NO generation from non-stimulated whole blood phagocytes and macrophages, resp., but suppressed OZP-(opsonized zymosan particles)-activated ROS generation, LPS-induced iNOS expression and NO production. This dual mode of action suggests their anti-inflammatory activity, which is known for silver linden extracts. PSI expressed the highest complement fixation and macrophage-stimulating activities and was active on intestinal Peyer's patch cells. PSIII was active on non-stimulated neutrophils, as it induced β_2-integrin expression, revealing that acetylated and highly glucuronidated RGI exhibits immunomodulating properties via phagocytes.

© 2017 Elsevier Ltd. All rights reserved.

Abbreviations: AGII, arabinogalactan type II; AUAC, anhydrouronic acid content; BSA, bovine serum albumin; CD18, marker for β_2-integrin; CD62L, marker for L-selectin; CL, chemiluminescence; DA, degree of acetylation; DM, degree of methoxylation; DSS, sodium 4,4-dimethyl-4-silapentane-sulfonate; fMLP, N-Formylmethionyl-leucyl-phenylalanine; FTIR, Fourier transform infrared; GlcA-RGI, glucuronidated RGI; HBSS, Hank's buffered salt solution; HG, homogalacturonan; IC_{50}, a concentration giving 50% hemolysis of erythrocytes; iNOS, inducible nitric oxide synthase; KDO, 3-deoxy-D-manno-2-octulosic acid; LDH, lactate dehydrogenase; Linden PSC, crude polysaccharide complex from *Tilia tomentosa*; Linden PSin70, obtained from linden PSC after an exhaustive ethanol treatment; LPS, lipopolysaccharides; NMR, Nuclear magnetic resonance; NO, nitric oxide; OZP, opsonized zymosan particles; PBS, phosphate-buffered saline; PMA, phorbol 12-myristate 13-acetate; PP, Peyer's patches; PSI-PSIII, polysaccharide fractions I, II, and III obtained after anion-exchange chromatography from linden PSin70; RGI and II, rhamnogalacturonan type I and II; ROS, reactive oxygen species; SRBC, sheep red blood cells; WBP, whole blood phagocytes.

* Corresponding author at: Laboratory of Biologically Active Substances, Institute of Organic Chemistry with Centre of Phytochemistry, Bulgarian Academy of Sciences, 139 Ruski Blvd., BG-4000, Plovdiv, Bulgaria. Tel./Fax.: +359 32 64 27 59.
E-mail address: lbas@plov.omega.bg (M.G. Kratchanova).

http://dx.doi.org/10.1016/j.carbpol.2017.07.073
0144-8617/© 2017 Elsevier Ltd. All rights reserved.

1. Introduction

Tilia genus (Tiliaceae) comprises around 45 species of deciduous trees, which are native to the Northern hemisphere, as silver linden (*T. tomentosa*, syn. *T. argentea*) forms coenoses only in the Balkans (Hritcu & Cioanca, 2016; Radoglou, Dobrowolska, Spyroglou & Nicolescu, 2009). Linden (lime tree, basswood or "lipa" in Slavic) is famous in the European mythology, literature, folklore and medicine. Since the middle ages, the linden flower tea has been used as a diaphoretic to promote perspiration. The traditional use of the linden blossom is for common cold, feverish colds, cold-related coughs, catarrhs, mental stress, high blood pressure, headache, indigestion, diarrhea, skin ailments, etc (Chinou, 2012a; WHO, 2010). *Tilia* flos (*T. cordata*, *T. platyphyllos*, *T. vulgaris*) is included in the European Pharmacopeia and approved by the German Commission E for internal use for colds and cold-related coughs. It is listed by the Council of Europe as a natural source of food flavouring and with GRAS status from FDA. *T. tomentosa* buds are popular and used worldwide for preparation of tea and dietary supplements, such as the commercially available "silver linden bud extract" used in gemmotherapy (Allio et al., 2015). The largest suppliers of the vegetal product now are China, Bulgaria, Poland, Russia, Romania and Turkey (Hritcu & Cioanca, 2016).

The active constituents in the linden inflorescences are flavonoids, phenolic acids, tannins, essential oils, mucilage, triterpenes and sterols (Hritcu & Cioanca, 2016; Kosakowska et al., 2015). There are not many studies on the biologically active constituents of *T. tomentosa* blossom, except for its flavonoids having anti-inflammatory activity (Chinou, 2012b; Matsuda, Ninomiya, Shimoda, & Yoshikawa, 2002; Viola et al., 1994). It is found that the mucilage is the main component of the linden flower bracts and it is also detected in the subglandular parenchyma tissue of sepals (Hritcu & Cioanca, 2016). The traditional use of the linden mucilage is related to its emollient properties and antitussive activity, but many of its immunomodulating compounds, such as the anti-inflammatory constituents are unknown (Hritcu & Cioanca, 2016). It has been reported that *Tilia* flower mucilage is rich in pectic polysaccharides, however their structural diversity and biological activity are little studied. Kram and Franz (1983, 1985), and Yakovlev (1985) found that pectins are abundant in *Tilia cordata* blossoms. Earlier, Simson and Timell (1978) found that a cambial tissue from basswood, *T. americana*, contains 50–60% pectin. The immunomodulating activity of the linden blossom is attributed to its flavonoids (tiliroside, rutin), coumarins (scopoletin) and monoterpenes, but there are not such studies on the linden pectins (Arcos et al., 2006; Manuele, Ferraro, & Anesini, 2008; Matsuda et al., 2002). Interestingly, aqueous extracts from linden flowers, which should contain pectins, have shown *in vitro* stimulatory effects on lymphocyte proliferation and antitumor activity (Brizi, Marrassini, Zettler, Ferraro, & Anesini, 2012). In search of the mucilaginous effect on irritated buccal membranes, Schmidgall, Schnetz, and Hensel (2000) showed that a raw polysaccharide complex from the flowers of *T. cordata* expresses a moderate bioadhesion to epithelial tissue *ex vivo*.

Pectic polysaccharides contain three main building blocks covalently linked together – unbranched homogalacturonan (HG), ramified RGI and II. The linear HG is methyl-esterified and O-acetylated to different extent. RGI is also acetylated but branched at C-4 of the L-Rha residues with side chains of α-(1 → 5)-L-arabinans, β-(1 → 4)-D-galactans, arabinogalactan (AG) type I and II (Ridley, O'Neill, & Mohnen, 2001; Schols & Voragen, 2002). The AG structural motifs are extremely important for the expression of immunomodulating activity. This could clearly be seen from the works of Yamada & Kiyohara on pectic polysaccharides isolated from the Japanese Kampo medicine formulations and Paulsen and coworkers on pectins from Malian medicinal plants (Paulsen & Barsett, 2005; Wangensteen, Diallo, & Paulsen, 2015; Yamada & Kiyohara, 2007). RGII is composed of a partly methyl-esterified galacturonan backbone, carrying four oligosaccharide side chains rich in rare sugars (2-Me-Fuc, 2-Me-Xyl, Api, Kdo and Dha) (Ridley et al., 2001). Pectins have beneficial effects on the immune, digestive, excretory, cardiovascular, endocrine, nervous and respiratory systems (Groudeva, Kratchanova, Panchev, & Kratchanov, 1997; Fan et al., 2012; Liu, Dong, Yang, & Pan, 2016; Šutovská, Capek, Fraňová, Pawlaczyk, & Gancarz, 2012; Xie, Zhang, & Zhang, 2015; Yamada & Kiyohara, 2007). The pectic polysaccharides exhibit moderate immunomodulating effects against T-cells, B-cells, NK-cells, neutrophils, macrophages, dendritic cells, thrombocytes and abnormal tumor cells (Bijak et al., 2013; Holderness et al., 2011; Inngjerdingen et al., 2007; Inngjerdingen et al., 2008; Ma et al., 2013; Yamada & Kiyohara, 2007). These actions combined with their regulatory effects on immune signaling proteins, complement system and probiotic bacteria could be useful for prevention and supplementary therapy of infectious, tumor, gastrointestinal and inflammatory diseases.

In our preliminarily study a crude polysaccharide complex from *T. tomentosa* (linden PSC) expressed *ex vivo* immunomodulating activity against human phagocytic leukocytes, T-cells, murine Peyer's patch cells and anti-tumor activity *in vitro* (Georgiev et al., 2017). The aim of the current study is to characterize the chemical diversity and immunomodulating properties of purified pectic polysaccharides from *T. tomentosa* Moench blossoms. This will help in elucidation of the structure-activity relationship of these possible pharmacologically active linden constituents.

2. Materials & methods

2.1. Plant material

Linden flowers were collected in June 2013 in Plovdiv (Bulgaria), air-dried for two weeks and stored in a desiccator until use. The plant material was identified as silver linden, *Tilia tomentosa* Moench (Tiliaceae), by Dr. Evgeny Tsavkov from the Department of Dendrology in the University of Forestry, Sofia. A voucher specimen (SOA061426) was deposited in the Herbarium of the Agricultural University of Plovdiv.

2.2. Isolation and purification of silver linden flower polysaccharides

Linden PSC was extracted with boiling water as previously described (Georgiev et al., 2017).

The linden PSC was dissolved in water (10 mg/ml) and precipitated twice with 95% ethanol (24 h each) with a final alcohol concentration of 70%. This step was for partly removing of smaller molecules. After each run polysaccharide precipitates were separated by centrifugation at 4000 rpm for 30 min at 20 °C. Then, the recovered highest in yield (47.1% on linden PSC basis) polysaccharide-containing fraction insoluble in 70% ethanol (linden PSin70) was applied to a DEAE-Sepharose FF column (1.5 × 50 cm) in HCO^-_3 form, coupled with a FPLC BioLogic® LP system (BioRad). The column was eluted successively with 170 ml water, then with 300 ml of: 0.35 M NH_4HCO_3; 0.45 M NH_4HCO_3 and 1.0 M NH_4HCO_3, at 1 ml/min flow rate. Three pectic polysaccharide fractions PSI-PSIII were obtained, as 7 ml fractions were collected and peaks were visualized by the phenol-sulfuric acid (not shown) and *m*-hydroxydiphenyl methods (Dubois, Gilles, Hamilton, Rebers, & Smith, 1956; Blumenkrantz & Asboe-Hansen, 1973). The samples were concentrated under vacuum, dialyzed against water (MWCO 12–14 kDa, 72 h at 4 °C), filtered through 0.2 μm cellulose nitrate filters (Sartorius), freeze-dried and stored in a desiccator in dark.

2.3. General methods

Total amount of sugars was quantified by the phenol-sulfuric acid method, using 1:1 mixture of glucose and galacturonic acid as a standard (Dubois et al., 1956). Anhydrouronic acid content (AUAC) was determined by the *m*-hydroxydiphenyl method, using galacturonic acid as a standard (Blumenkrantz & Asboe-Hansen, 1973). Degree of methoxylation (DM) was determined after methanol release with 0.5 M NaOH and its further oxidation to formaldehyde by alcohol oxidase (*P. pastoris*, Sigma-Aldrich), and measuring of the absorbance of the obtained colored product with Purpald® (Sigma-Aldrich) at λ = 550 nm (Anthon & Barrett, 2008). Degree of acetylation (DA) was measured according to McComb and McCready (1957), using β-D-glucose pentaacetate as a standard. Molecular weight was determined by HPSEC-RID (Waters) with Shodex standard P-82 kit (pullulan standards, Showa DENKO, Tokyo, Japan) (Georgiev, Ognyanov, Yanakieva, Kussovski, & Kratchanova, 2012). The elution profile of PSIII (1.9 mg/1 ml) was also analyzed by FPLC on a Sephacryl S300 column (100 × 1.5 cm) at a flow rate of 0.5 ml/min 0.2 M NaCl and 5 ml fractions were collected. Protein content (BSA standard) was analyzed according to Bradford (1976). Only distilled water was used for all experiments.

2.4. Monosaccharide composition and glycosidic linkage determination

Polysaccharide samples (1 mg) with added 100 μg mannitol as an internal standard were subjected to methanolysis with anhydrous 3 M HCl in methanol for 24 h at 80 °C. The formed methyl glycosides of different monosaccharides were converted into their corresponding TMS derivatives and analyzed by GC-FID on a Focus GC system (Thermo Scientific, Milan, Italy), according to Chambers and Clamp (1971) and Barsett, Paulsen, and Habte (1992). The presence of KDO (3-deoxy-D-manno-2-octulosic acid) was detected by the thiobarbituric acid assay, as modified by York, Darvill, McNeil, and Albersheim (1985).

Glycosidic linkage composition of PSI and PSIII (2 mg) were examined by the methylation approach. Prior to methylation uronic acids in the polysaccharides were reduced with $NaBD_4$ to 6,6′-dideuterio-sugars that could be differentiated from the neutral sugars (Kim & Carpita, 1992). The procedure was completed by methylation, acid hydrolysis and preparation of alditol acetates, partly as described by Ciucanu and Kerek (1984). First hydrolysis was performed with 2.5 M TFA for 2 h at 100 °C. Secondly, only for PSIII (2 mg) formolysis with 90% HCOOH (1 ml) for 6 h at 120 °C and a further hydrolysis by addition of 5 ml water for 1 h at 100 °C was carried out on the methylated polymer. This was necessary for the complete hydrolysis of the glycosidic bonds in PSIII. The partly methylated alditol acetates were analyzed by a GC-EI/MS-QP2010 system (Shimadzu, Kyoto, Japan), coupled with a Restek Rxi-5MS column (30 m, 0.25 mm i.d., 0.25 μm film) in a Scan mode (40–450 ions), as described by Ho, Zou, Aslaksen, Wangensteen, and Barsett (2016). The detection and quantification of the relative amounts of each glycosidic linkage type was based on the chromatographic behavior (RT), ionization patterns and results from the monosaccharide composition.

The presence of AGII was detected by precipitation with the ß-glucosyl Yariv reagent (Van Holst & Clarke, 1985).

2.5. Contamination with microbial lipopolysaccharides (LPS)

Eventual LPS contamination was checked by a possible detection of 3-hydroxy fatty acids as their specific chemical markers in the form of acetylated fatty acid methyl esters on the GC-EI/MS-QP2010 system (Shimadzu, Kyoto, Japan), coupled with the Restek Rxi-5MS column (30 m, 0.25 mm i.d., 0.25 μm film) in a SIM mode (257 ion intensity for calculation), as described by de Santana-Filho et al. (2012) and Ho et al. (2016).

2.6. Nuclear magnetic resonance (NMR) spectroscopy

PSIII (12 mg) was dissolved in D_2O, freeze-dried, re-dissolved in 700 μl D_2O and 500 μl sample was used. 1D ^1H, ^{13}C and 2D $^{13}C/^1H$ HSQC, $^1H/^1H$ COSY 90, $^1H/^1H$ TOCSY, $^1H/^1H$ ROESY, $^{13}C/^1H$ HMBC, $^{13}C/^1H$ HSQC-NOESY experiments were performed on a Bruker Avance III HD Ascend 800 MHz spectrometer operating at 800.03 MHz (Bruker, Fällanden, Switzerland) with the software Bruker TopSpin™ 3.5 at a temperature of 333.15 K. The chemical shifts were referenced to an internal standard DSS (sodium 4,4-dimethyl-4-silapentane-sulfonate).

2.7. Fourier transform infrared (FTIR) spectroscopy

FTIR spectra of PSIII before and after saponification with NaOH were obtained on a Nicolet™ FTIR spectrometer (Thermo Fischer Scientific, USA) controlled by the OMNIC 3.2 software. The sample was pressed onto the attenuated total reflectance (ATR) crystal using a high pressure tower to provide consistent results. No more than 2 mm^3 of the sample was used to cover the ATR diamond cell.

2.8. Small-angle X-ray scattering (SAXS)

SAXS experiments of PSIII aqueous solutions in different concentrations and at different temperatures were carried out using a Bruker Nanostar instrument (RECX-Norway, Cu-Kα radiation λ = 1.54 Å). The instrument setting allows to access a Q-range between 0.009 $Å^{-1}$ to 0.2 $Å^{-1}$, where Q is defined by $Q = 4\pi\sin(\theta/2)/\lambda$, as θ is the scattering angle and λ the wavelength. The samples were measured in a Quartz cell of 1 mm path length. The data were analysed on an absolute scale (water as a primary standard), using a coexistence model of a linear polymer chain:

$$I(Q) = I_{cluster}(Q) + I(Q)_{chain}$$

where the contribution from the dissolved polymer chains can be written as:

$$I(Q)_{chain} = \frac{\varphi M_w}{d_p}(\rho_p - \rho_0)^2 P(Q)_{chain}$$

Here φ is the volume fraction of a polymer, M_w is the weight average molecular weight, $d_p = 1.2$ g/ml is the density for typical hydrogen-bonding polymers (Sommer, Pedersen, & Stein, 2004), ρ is the electron density for the solvent, $\rho_0 = 9.4 \times 10^{10}$ cm^{-2} and the polymer ($\rho_p = 1.1 \times 10^{11}$ cm^{-2}). $P(Q)_{chain}$ is the form factor derived by Beaucage (1996):

$$P(Q)_{chain} = \exp\left(-\frac{Q^2R_g^2}{3}\right) + \frac{d_f}{(QR_g)^{d_f}}\Gamma\left(\frac{d_f}{2}\right)\cdot\left(\frac{\left[erf\left(\frac{Q\cdot Rg}{\sqrt{6}}\right)\right]^3}{Q}\right)^{df}$$

where R_g is the radius of gyration, d_f is the fractal dimension ($d_f = 2.0$, 1.7 for θ and a good solvent, respectively). Γ(x) is the gamma function and erf(x) is the error function. The cluster contribution can be taken into account by the term:

$$I(Q)_{blob} = \frac{C}{(1 + Q^2\xi^2)^2}$$

where ξ is the characteristic size of the cluster (correlation length), and C is a numerical constant.

2.9. Immunomodulatory effect

2.9.1. Ethics

Blood sampling procedure was in accordance with the Helsinki Declaration of 1975, as revised in 1983. Animal experiments were approved by the Animal Research Committee of the Kitasato University, and performed in accordance with the Guidelines for Care and Use of Laboratory Animals at the Kitasato University and the National Research Council Guide for the Care and Use of Laboratory Animals in Japan.

2.9.2. Animal procedure and care

Female C3H/HeJ mice (6–8 weeks old) were purchased from Japan SLC (Shizuoka, Japan), and male ICR mice (4 weeks old) were from Charles River (Tokyo, Japan). The mice were housed in plastic cages in an air-conditioned room at 23 ± 2 °C with a relative humidity of 55 ± 10% under a 12 h-light-dark cycle, and fed a standard laboratory diet with water given *ad libitum*.

2.9.3. Complement fixation assay

The inhibition of complement hemolysis (complement fixation) of target antibody sensitized sheep red blood cells (SRBC) by a normal human serum pre-treated with PSI, II or III was performed according to Michaelsen, Gilje, Samuelsen, Høåsen, and Paulsen (2000) (Method A). A highly active pectic polysaccharide BP-II from the aerial parts of *Biophytum petersianum* was used as a positive control (Grønhaug et al., 2011). The complement fixation activity induced by the test samples was calculated on the basis of a colorimetric measurement of hemoglobin released from lysed SRBC after incubation with a normal human serum pretreated with PSI, II or III by the formula: $[A_{control} - A_{test}]/A_{control} \times 100\%$. From these data a dose-response curve was constructed and the concentration of a test sample giving 50% inhibition of lysis (IC_{50}) was calculated. The results are obtained from two independent experiments.

2.9.4. ROS production from human whole blood phagocytes (WBP) and isolated neutrophils

Heparinized (50 IU/ml) blood samples were obtained from the cubital vein of healthy human volunteers after overnight fasting. The isolation of human neutrophils from venous blood was accomplished according to the procedure of Nauseef (2014). Kinetics of ROS production by WBP and isolated neutrophils was analyzed by luminol-enhanced chemiluminescence (CL) for a period of 60 min at 37 °C, using 96-well white flat bottom culture plates on a luminometer (Orion II Berthold Detection Systems GmbH, Germany). The principle of the method was previously described (Vasicek, Lojek, Jancinova, Nosal, & Ciz, 2014). Briefly: 25 μl of ten times diluted blood with Hank's buffered salt solution (HBSS) or 0.2×10^6 cells/well of isolated neutrophils in phosphate-buffered saline (PBS) were mixed with 25 μl 1 mM luminol (10 mM stock solution in 0.2 M borate buffer) HBSS solution and incubated with HBSS solutions of PSI, II or III (50 and 100 μg/ml) for spontaneous (non-stimulated with known activators) CL. Furthermore, 12.5 μl or 5 μl of ten times diluted blood (or 0.2×10^6 cells/well) mixed with 25 μl luminol were used for incubation of each linden polysaccharide with 25 μl (0.5 μg/ml) phorbol 12-myristate 13-acetate (PMA-activated, Sigma-Aldrich) or 25 μl (62.5 μg/ml) OZP (OZP-activated). The final volume for spontaneous, PMA- and OZP-activated CL tests was 250 μl. PMA and OZP were used as ROS production activators. The recorded values included the intensity of CL emitted during the time interval studied (integral of CL). The results are expressed as percentage of the control (mean ± SEM) from five independent experiments.

2.9.5. Determination of the cell surface expression of adhesion molecules

The measurements were performed according to the method previously described (Gallova, Kubala, Ciz, & Lojek, 2004). Briefly, human neutrophils (1×10^5 cells) were incubated in plastic tubes (Falcon, USA) with PSI, II or III (100 μg/ml) for 1 h and with the activators fMLP (N-formyl-met-leu-phe, 0.1 μM) and PMA (0.01 μg/ml) for 10 min. After the incubation anti-CD18 (anti-β_2-integrin) and anti-CD62L (anti-L-selectin) monoclonal antibodies (5 μl of each) were added. The samples were incubated at 4 °C for 15 min, subsequently centrifuged, re-suspended in PBS and analyzed by a flow cytometer FACSVerse™ (Becton Dickinson, USA). The median fluorescence intensity was determined and corrected for unspecific staining by subtracting the fluorescence of cells stained with the control antibody (isotype control). The data are expressed as $CD62L^-/CD18^+$ population (mean% of total leukocytes ± SEM) from five independent experiments.

2.9.6. Nitric oxide (NO) production from murine macrophages

Murine macrophages cell line RAW 264.7 (ATCC, USA) were incubated in 12-well flat bottom culture plates at 1×10^5 cells/well with PSI, II or III (50 and 100 μg/ml) alone in DMEM-high Glc supplemented with 10% (v/v) FBS and 1% (v/v) penicillin/streptomycin (500 μl final volume) (HyClone™, GE Healthcare Life Sciences) growth medium for 24 and 48 h at 37 °C and 5% CO_2. The cells were also incubated with polysaccharides in combination with 10 ng/ml LPS (*E. coli*/026:B6, Sigma-Aldrich). The generation of NO was determined indirectly as the accumulation of nitrites in the cell culture supernatant. At the end of the incubation period, the culture media were collected and centrifuged at 16 000×*g*, 4 °C for 10 min. Then, 150 μl of supernatants were mixed with equal volumes of the Griess reagent (Sigma-Aldrich) in a 96-well plate and the mixtures were incubated at room temperature for 30 min in dark. The absorbances were measured at 546 nm and $NaNO_2$ (0–52 μM) was used as a standard (Lojek et al., 2011). The results are expressed as mean ± SEM from three independent experiments.

2.9.7. Western blot analysis of inducible nitric oxide synthase (iNOS)

RAW 264.7 cells, which were obtained as described in 2.9.6., were lysed in the lysis buffer (1% SDS, 0.1 M Tris pH 7.4, 10% glycerol, 0.001 M sodium *o*-vanadate, 0.001 M PMSF). The protein concentrations were determined by using the BCA™ protein assay (Pierce, USA), with BSA as a standard. Equal amounts of protein (18 μg) were then subjected to SDS-PAGE using a 10% separating gel. The expression of iNOS protein was quantified by a Western blot analysis (Pekarova et al., 2011). Anti-iNOS/NOS Type II mouse monoclonal antibody (Cell signaling Technology, 1:5000) and ECL™ anti-rabbit IgG horseradish peroxidase linked whole antibody (from goat; Cell Signaling Technology, 1:2000) were used. The immunoreactive bands were detected using the ECL™ detection kit (Pierce) and exposed to a radiographic film (AGFA). The relative protein levels were measured by scanning densitometry using the ImageJ™ programme, and the individual band density value was expressed in arbitrary units. The results are expressed as mean ± SEM from three independent experiments.

2.9.8. Cytotoxicity assay

Cytotoxicity was estimated by lactate dehydrogenase (LDH) activity in the cell culture supernatant of RAW 264.7 cells, as obtained in 2.9.6., using the LDH Cytotoxicity Detection Kit^{PLUS} (Roche Applied Science, Switzerland). The results are expressed as mean ± SEM from three independent experiments.

2.9.9. Immunomodulating activity against murine Peyer's patch (PP) cells

Immunomodulating activity was measured by the enhanced production of bone marrow cell-proliferative cytokines from PP cells of specific pathogen-free C3H/HeJ mice ($Tlr4^{Lps-d}$) according to Hong, Matsumoto, Kiyohara, & Yamada (1998). Suspensions (1.2×10^6 cells/ml, 180 μl) of the PP cells (5–9 patches obtained per mouse) from the small intestine of C3H/HeJ mice were cultured with H_2O (negative control), AMOL-1 (pectic polysaccharide from *Astragalus mongholics* as a positive control, Kiyohara et al., 2010) or 100 μg/ml of the polysaccharide fractions (PSI, II or III, 20 μl) in a 96-well flat bottom culture plate (FALCON 3072) for 6 days at 37 °C in a humidified atmosphere of 5% CO_2–95% air. The resulting culture supernatants (50 μl) were further cultured with a bone marrow cell suspension (5.0×10^5 cells/ml) from male ICR mice for 6 days. The number of proliferated bone marrow cells was measured by Alamar Blue™, as described previously (Hong et al., 1998). The results are shown as mean ± SEM.

2.9.10. Tumor cell growth inhibition in vitro

Growth inhibitory effect of some of the linden polysaccharides was studied against FL cell line (ATCC CCL 62, NBIMCC 94) derived from normal human amniotic cells and different human tumor cell lines: A549 (ATCC CCL 185), LS180 (ATCC CL-187), HT29 (ATCC HTB-38), HeLa (ATCC CCL-2), CaOV (NBIMCC 1108), Jurkat (ATCC, TIB-152) and MOLT-4 (ATCC, CRL-1582). The studied cell lines were treated with PSI or III (50 and 25 μg/ml) for 24, 48 and 72 h, and the cell viability was tested with the MTT (3-(4,5-dimethylthiazol-2-yl)-2,4-diphenyltetrazolium bromide) (Sigma-Aldrich) reagent as previously described (Georgiev et al., 2017). The percent inhibition of the cell growth was calculated using the mean absorbance units from each test sample and the mean data from the control cells incubated in the absence of linden polysaccharides. The samples were analyzed in triplicates.

2.10. Statistical analysis

The statistical significance was analyzed by the Student's *t*-test, using the Statview software (SAS Institute, Inc.). The mean ± SEM were compared to those from the control. Values of $p < 0.05$ were considered as statistically significant.

3. Results

3.1. Purification and structural characterization of the linden polysaccharides

3.1.1. Purification and chemical composition of the linden polysaccharide fractions

The linden PSin70 fraction (AUAC = 43.4%) was subjected to anion-exchange chromatography on a DEAE-Sepharose FF ($-HCO_3^-$) column and three defined acidic polysaccharide fractions PSI-III were obtained by a stepwise elution with 0–1 M NH_4HCO_3 (Fig. S1). After sample loading the column was eluted with 170 ml water, but this gave no neutral fractions. We did not find any further carbohydrate-containing fractions when the column was successively washed with 2 M NaCl after the stepwise elution. In Table 1 results from the chemical characterization of the obtained three pectic fractions are presented. The combined yield of the studied samples is 42.7% and it is 20.2% and 1.25% from the linden PSC and dried *T. tomentosa* flowers, respectively. The results from the AUAC analysis (39.9-46.8%) of the samples show that the isolated polysaccharides have acidic character. Kram and Franz (1983) reported between 10 and 63% AUAC in the obtained four acidic fractions from *T. cordata* flowers. Methoxyl esters are detected only in PSI, which is found to be a low methoxylated pectin with DM = 13.1%. The total acetyl content in the three fractions varies between 0.6-3.3%, as PSII and PSIII are characterized with higher acetyl content than PSI, which indicates that these fractions are considerably acetylated. The three polysaccharide samples contain all monosaccharides typical for pectins and also small amounts of Glc and Man. Interestingly, the Rha content is high in all fractions, originating from the high Rha content (11.5%) in the linden PSC for which was shown by a FTIR analysis that it is rich in RGI backbone structures (Georgiev et al., 2017). The values for Rha and GalA in PSII and III are in the same range. Theoretically, the ratio GalA:Rha in the RGI backbone tends to be 1:1, as this ratio for PSI, II and III is 6.2, 1.3 and 1.1, respectively. According to Denman and Morris (2015) the difference between GalA and Rha could give the approximate content of HG (%) in pectins. For PSI the HG content is estimated to be 57%, following 8.3% for PSII and 2.0% for PSIII. It was calculated that GlcA is 30–31% from the uronides in the linden PSC on the basis of colorimetric and chromatographic determination of both uronic acids (Georgiev et al., 2017). Interestingly, the GlcA content is high in PSII and III, compared to the other monosaccharides present. Generally, GlcA and/or 4-O-Me-GlcA are presented in minor amounts linked to the AG side chains, thus expected to be lower than Gal + Ara (Ridley et al., 2001). This is the case in PSI but it is not the same for PSII and III. Additionally, GlcA:Rha ratio is 0.7 and 1.0 for II and III, which shows that the uronic acid is not a rare substituent in our RGI. PSI appears to be a typical pectic polymer with high HG content, PSII and III are unusual RGsI, due to the high content of GlcA. The gross calculation for the glucuronic acid-containing polymers indicates that they are presented in more than 0.7% in the dried flowers.

PSI has a considerably lower M_w (28.2 kDa) than PSII and III – 949 and 382 kDa, respectively. Furthermore, PSIII was eluted as a single peak with 0.2 M NaCl on a Sephacryl S300 column and its molecular weight was determined to be 352 kDa, using pullulan calibration standards (0.59×10^4–40.4×10^4 Da). This value is in the range between M_w and the number average molecular weight M_n calculated for PSIII from the HPSEC-RID results (Table 1). The polydispersity index M_w/M_n for PSII and PSIII is 1.39 and 1.22, respectively. The thiobarbituric acid assay shows the presence of KDO in PSI, which is used as an indicator for presence of RGII. The specific immunodiffusion with the *β*-glucosyl Yariv reagent for detection of 3,6-galactans or AGII is positive only for PSI and II. PSI is distinctive with the highest content of Ara and Gal, followed by PSII. The isolated linden pectins are also characterized by a very low protein content <1.0%.

The three purified pectic fractions (PSI-PSIII) were tested for the presence of LPS, which are considered to be contaminants during the purification procedure by detection of some characteristic LPS fatty acid constituents using GC–MS analysis. It appears that there is no LPS contaminants in these polysaccharide fractions because the LPS marker 3-hydroxy tetradecanoic acid (3-OH-$C_{14:0}$) was not detected (de Santana-Filho et al., 2012).

3.1.2. Linkage determination

In Table 2 are shown the results for estimation of the linkage composition in PSI and III. Based on the quantitative linkage results, we found that PSI is composed predominantly of 1,4-linked Gal*p*A (59.4%) and 1,2-linked Rha*p* (8.4%) with a minor amount of 1,2,4-linked Rha*p* (1.4%) most probably substituted with arabinans and highly branched AGs with AGII structural characteristics. This means that PSI contains mainly HG and RGI structures. These findings are in a good agreement with the calculated HG content according to Denman and Morris (2015) and the Yariv's test for AGII. It is estimated that the 1,2,4-linked Rha*p* is 12.7% from the total Rha in PSI (Table 2). The presence of 1,3,4-linked Gal*p*A units in both samples is not unusual and it could be an indicator for RGII structures and other substituted galacturonans, such as xylogalac-

Table 1
Yields and chemical characterization of silver linden pectic fractions obtained after anion-exchange chromatography of linden PSin70.

	PSI	PSII	PSIII
Yield [% of linden PSC]	9.0	2.6	8.6
Yield [% of linden PSin70]	19.1	5.4	18.2
Yield [% of dried flowers]	0.56	0.16	0.53
Total sugars[a] [%]	55.2	67.5	64.8
AUAC [%]	46.8	39.7	39.9
DM[b] [mol%]	13.1	n.f.	n.f.
(Methoxyl content [%])	(1.1)		
Acetyl content [%]	0.6	3.3	2.9
Protein content [%]	0.4	n.d.	0.5
LPS [%]	n.f.	n.f.	n.f.
Monosaccharide composition [w/w%]			
Ara	7.5[c] (9.2)[d]	2.3 (2.7)	1.9 (2.2)
Rha	11.0 (12.3)	29.2 (32.3)	29.8 (33.1)
Fuc	trace	trace	trace
Xyl	1.9 (2.3)	0.9 (1.1)	1.0 (1.2)
Man	0.1 (0.1)	0.4 (0.4)	0.2 (0.2)
Gal	6.7 (6.8)	4.7 (4.8)	3.4 (3.5)
Glc	3.3 (3.4)	3.6 (3.6)	2.2 (2.3)
GlcA	1.6 (1.5)	21.4 (20.0)	29.6 (27.8)
GalA	67.9 (64.3)	37.5 (35.1)	31.8 (29.8)
Kdo	+	n.d.	n.d.
AGII	+	+	n.f.
Molecular weight [Da]	2.82×10^4	9.73×10^5 (68.0%)	3.91×10^5 (78.3%)
		1.31×10^5 (14.7%)	5.05×10^4 (15.4%)
(M_w)[e]		0.14×10^4 (17.3%)	0.14×10^4 (6.3%)
(M_n)[f]		(9.49×10^5)	(3.82×10^5)
		(6.81×10^5)	(3.14×10^5)

n.f. – not found; n.d. – not determined.
[a] Mixture of 1:1 Glc:GalA was used as a standard.
[b] Calculated on the AUAC basis, moles of methoxyl groups per 100 mol of GalA.
[c] w/w%, calculated on the total carbohydrate content basis.
[d] mol% of the total carbohydrate content.
[e] Weight average molecular weight.
[f] Number average molecular weight.

Table 2
Glycosidic linkage composition of two linden pectic fractions obtained after anion-exchange chromatography of linden PSin70.

Glycosidic linkages	PSI[c]	PSIII[d]
T-Ara*f*	3.4[a] (4.2)[b]	–
1,3-Ara*f*	0.3 (0.4)	–
1,5-Ara*f*	3.0 (3.6)	–
1,3,5-Ara*f*	0.8 (1.0)	–
T-Rha*p*	1.2 (1.4)	–
1,2-Rha*p*	8.4 (9.4)	29.8 (33.1)
1,2,4-Rha*p*	1.4 (1.6)	–
1,3-Fuc*p*	trace	–
1,4-Xyl*p*	1.9 (2.3)	–
T-Gal*p*	2.6 (2.6)	–
1,3- Gal*p*	0.9 (0.9)	–
1,6-Gal*p*	1.1 (1.1)	–
1,3,6-Gal*p*	2.1 (2.2)	–
1,4-Glc*p*	3.3 (3.4)	2.2 (2.3)
T-Glc*p*A	1.6 (1.5)	29.6 (27.8)
T-Gal*p*A	5.3 (5.0)	–
1,4-Gal*p*A	59.4 (56.2)	1.8 (1.7)
1,3,4-Gal*p*A	3.3 (3.1)	30.0 (28.1)

[a] w/w%, calculated on the total carbohydrate content.
[b] mol% of the total carbohydrate content.
[c] 2.5 M TFA for 2 h at 100 °C.
[d] 90% HCOOH for 6 h at 120 °C and further hydrolysis by addition of 5 ml d. water for 1 h at 100 °C.

turonans (Schols & Voragen, 2002). Normally, these fragments do not occupy high proportion in the initial not enzymatically treated pectins (Grønhaug et al., 2011). It could be stated that the 1,3,4-linked Gal*p*A in PSI might be related to RGII structures because this sample is KDO positive.

The methylated PSIII was subjected to formolysis in order to get a complete hydrolysis of the strong glycosidic bonds in this polysaccharide. Similar approaches have been applied for studying of other acidic polymers (Ohtani, Okai, Yamashita, Yuasa, & Misaki, 1995). After formolysis of the methylated PSIII, 30% of the 1,3,4-linked Gal*p*A units are obtained, which is in a comparable amount to that of the 1,2-linked Rha*p* (29.8%) and T-linked Glc*p*A (29.6%). The obtained 1:1:1 ratio of 1,2-Rha*p*:1,3,4-Gal*p*A:T-Glc*p*A reveals that the Glc*p*A monomers are O-3-bound to the Gal*p*A units in RGI. The ratio 1,4-linked Gal*p*A:(1,4+1,3,4)-linked Gal*p*A for PSIII from Table 2 gives a value of 5.7%, which shows that a minor amount of the GalA units are not O-3 glucuronidated. These GalA units could originate from HG structures. According to the polysaccharide classification, the glucuronidated RGI could be named a glucurono-rhamnogalacturonan I (GlcA-RGI) or an acetylated glucurono-rhamnogalacturonan I in this case.

Because of the low yield of PSII, it was not possible to be performed a linkage determination of this sample. PSII is characterized by a similar acetyl content to PSIII and a high GlcA content of 21.4%, therefore it is assumed that the Glc*p*A units might be also O-3 linked to the Gal*p*A.

3.1.3. NMR structural studies

On the basis of the monosaccharide, glycosidic linkage composition data and yield, PSIII was chosen for further detailed NMR analyses. One- and two-dimensional homo- and heteronuclear NMR experiments on a high-resolution 800 MHz spectrometer were performed in order to elucidate the structural features on the substitution of the GalA with GlcA and to localize the acetyl esters in PSIII. In Table 3 are presented ^{13}C and ^{1}H assignments found from COSY, TOCSY, ROESY, HSQC, HMBC and HSQC-NOESY spectra of PSIII, identified according to literature data and in accordance with the monosaccharide and glycosidic linkage compositions (Ravenscroft et al., 2015; Renard, Crépeau, & Thibault, 1999; Shakhmatov, Atukmaev, & Makarova, 2016; Sengkhamparn

Table 3
^{13}C and ^{1}H NMR chemical shift assignment (δ in ppm) of PSIII – acetylated glucurono-rhamnogalacturonan I, referenced to DSS.

Residue	C-1 H-1	C-2 H-2	C-3 H-3	C-4 H-4	C-5 H-5	C-6 H-6	CH_3CO
→4)-α-GalpA-3-OGlcpA-(1→2	100.3 5.02	70.1 4.10	81.3 4.20	80.3 4.66	73.5 4.77	176.2	
→2)-α-Rhap-(1→	101.3 5.25	79.3 4.11	72.2 3.87	74.7 3.42	71.8 3.71	19.2 1.24	
→2)-α-Rhap-3-OAc-(1→	101.3 5.37	70.4 4.20	– 5.09	78.2 3.61	72.8 4.11	19.2 1.28	22.9 2.09
β-GlcpA-(1→	106.6 4.71	76.4 3.49	78.4 3.52	74.3 3.61	78.2 3.81	177.1	

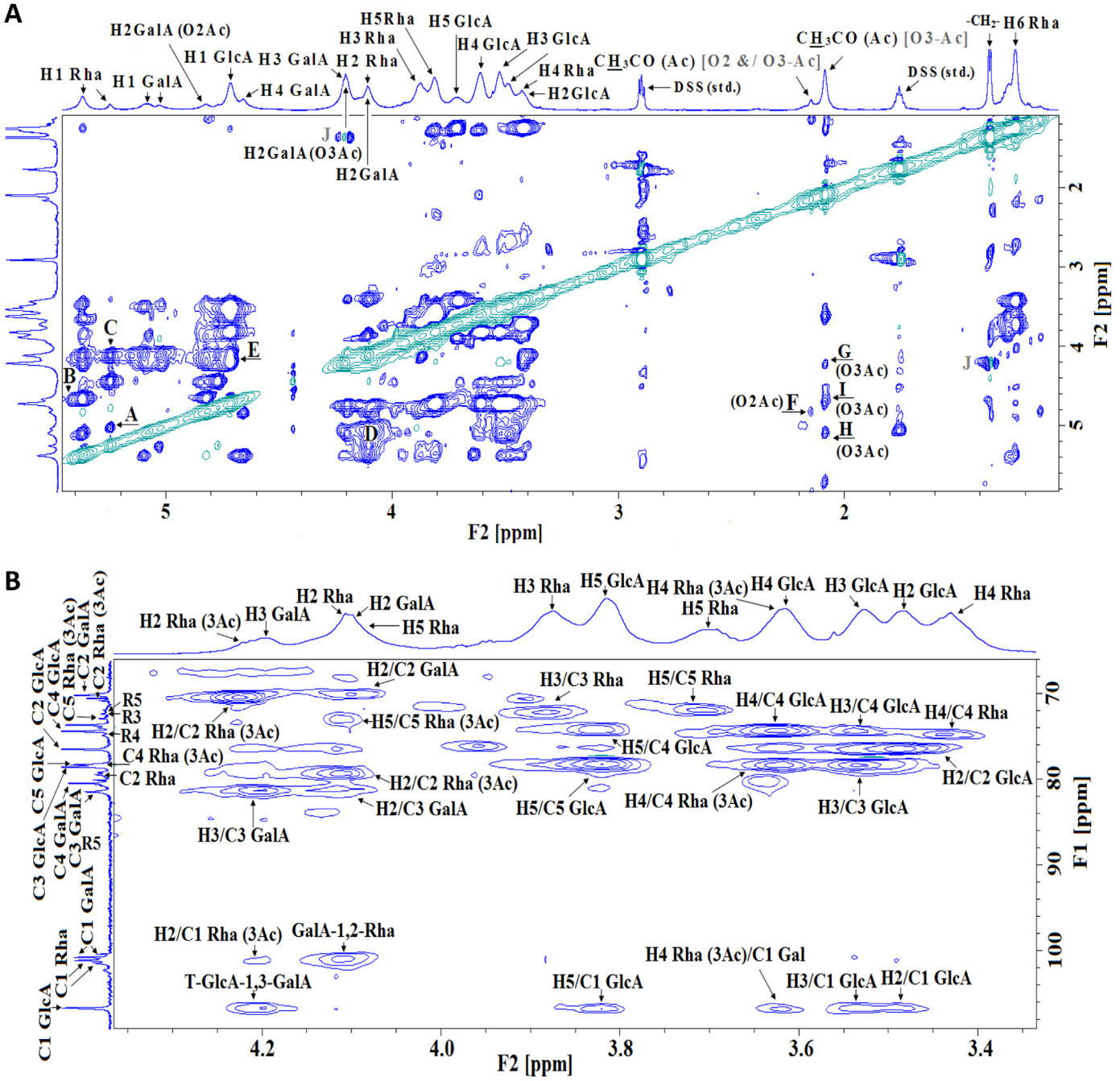


Fig. 1. 2D NMR analysis of linden pectic fraction PSIII. A) H^1/H^1 ROESY spectrum. Each letter (see section 3.1.3.) corresponds to important correlations. B) Partial $^{13}C/H^1$ HSQC-NOESY spectrum. R3-R5 are C3-C5 of the Rha residues.

et al., 2009; Shimizu & Tomoda, 1985). The absolute configurations were assumed to be the same as already found for RGI (McNeil, Darvill, & Albersheim, 1980). The detailed NMR study confirmed that PSIII is a GlcA-RGI, which is predominantly acetylated at O-3 of the α-L-Rha*p* units. The ROESY spectrum(Fig. 1A) reveals the following cross-peaks: H1 of α-L-Rha*p* and H1 of α-D-Gal*p*A residues at 5.25/5.02 ppm (**A**); H1 of internal α-L-Rha*p* with H4 of α-D-Gal*p*A units at 5.37/4.66 ppm (**B**); H1 of α-L-Rha*p* with H3 of α-D-Gal*p*A residues at 5.37/4.20 ppm (**C**); H2 of α-L-Rha*p* with H1 of α-D-Gal*p*A units at 4.11/5.02 (5.09) ppm (**D**). These correlations confirm the presence of the RGI backbone structure [→4)-α-D-Gal*p*A-(1 → 2)-α-L-Rhap-(1 → 4)-α-D-Gal*p*A-(1 →]$_n$ in PSIII. The absence of a correlation between H1 and H4 of α-D-Gal*p*A units confirms that the HG is really a minor part of the polymer.

More intriguing is a the through space cross-peak between H1 of terminally linked β-D-Glc*p*A units and H3 of 1,4-α-D-Gal*p*A residues at 4.71/4.20 ppm (**E**) in the ROESY spectrum (Fig. 1A). A correlation between C1 of β-D-Glc*p*A and H3 of 1,4-α-D-Gal*p*A at 106.6/4.20 ppm in the HSQC-NOESY spectrum is also found (Fig. 1B). This NMR information reveals that 1,4-α-D-Gal*p*A units in the RGI are O-3 substituted with β-D-Glc*p*A monomers. In fact, the chemical shifts for H2 (4.10 ppm), H3 (4.20 ppm) and H4 (4.66 ppm) of α-D-Gal*p*A, and H1 of 1,2-α-L-*R*ha*p* show markedly movement to the downfield region in comparison with literature data for pectins (Shakhmatov et al., 2016). This was also observed by Renard et al. (1999) and it indicates that α-D-Gal*p*A is substituted out of the RGI backbone and that the substitution influences the nearly located Rha. Beta anomeric configuration of Glc*p*A is suggested directly by the identified chemical shift of the H1 proton at 4.71 ppm (Renard et al., 1999).

The cross-peaks in the HSQC and HSQC-NOESY spectra for carbon and proton signals from methyl group of acetic acid ester at 22.9/2.09 ppm and 22.9/2.15 ppm are found, which confirms the presence of ester-linked acetic acid in PSIII. Correlations between the acetyl methyl protons and acetyl carbonyl carbons are observed in the C6 region of uronic acids in the HMBC spectrum. C6 signals of both uronic acid residues and $CH_3\underline{C}O$ group are overlapped. The presence of two peaks for $-\underline{C}H_3CO$ group at 2.09 ppm and 2.15 ppm suggests O-3 and O-2 acetylation in PSIII. The signal at 2.09 ppm is more intensive (integral ratio 2.09:2.15 ppm 3,8:1) and according to literature data attributed to O-3 acetylation of GalA in the HG, as well as of the Rha in RGI (Renard & Jarvis, 1999; Sengkhamparn et al., 2009). The proton methyl signal at 2.09 ppm is correlated with the peaks at 1.28 ppm (**F**), 3.61 ppm (**G**), 4.71 ppm (**H**) and 5.09 ppm (**I**) in the ROESY spectrum (Fig. 1A). The correlation **G** is the most intensive, supporting the closeness between the proton at 3.61 ppm with the acetyl protons. The correlation **F** indicates that the acetyl groups are within the Rha ring. The detailed analysis of the COSY, TOCSY, ROESY, HMBC and HSQC-NOESY spectra is in agreement with the predominant localization of the acetyl groups at O-3 of 1,2-α-L-*R*ha*p* units (Fig. 2). This is demonstrated by the downfield shift of H2 (4.20 pm), H3 (5.09 ppm), H4 (3.61 ppm) and H5 (4.11 ppm) of the 1,2-α-L-*R*ha*p* residues. By calculating the DA of PSIII on Rha basis instead of GalA basis, it is estimated that 33.3% of the Rha units are acetylated. The ratio between integral intensities of H6 of 1,2,-α-L-*R*ha*p*:1,2-α-L-*R*ha*p*-3OAc is 2.16:1, indicating that approximately 32% of the Rha units are acetylated. Similarly, Sengkhamparn et al. (2009) observed downfield shift of H2 (4.22 ppm), H3 (5.24 ppm) and H5 (3.91 ppm) of the O-3 acetylated 1,2,4-α-L-*R*ha*p* in pectin isolated from okra. Interestingly, *A. esculentus* (okra) belongs to Malvaceae family, where the linden was classified initially. The correlation between the resonances at 2.09 ppm and 4.71 ppm in the ROESY spectrum suggests that the proton at 4.71 ppm is conformationally close to the acetyl group. The monosaccharide composition and preliminarily glycosidic linkage analysis of PSIII indicate that it contains a small amount of Gal that might be linked to O-4 of 1,2-α-L-Rha*p*-3OAc. Therefore, it is proposed that the signal at 4.71 ppm contains the anomeric proton of T-β-D-Gal*p* units (Shakhmatov, Udoratina, Atukmaev, & Makarova, 2015). This is supported by the finding that the proton at 4.71 ppm (106.6 ppm) is adjacent to the proton at 3.52 ppm (74.3 ppm) in the COSY spectrum and by one cross-peak between 106.6 ppm and 3.61 ppm in the HSQC-NOESY spectrum (Fig. 1B).

The assignment of carboxyl carbonyl carbons C6 of both uronic acids was done from the HMBC spectrum, where the following information revealed, the proton H5 of 1,3,4-α-D-Gal*p*A at 4.77 ppm is correlated with the carbons at 176.2 ppm. Similarly, the H5 proton of β-D-Glc*p*A resonating at 3.81 ppm is connected with the carbons at 177.1 ppm. The absence of a signal at 53–55 ppm arising from $-O\underline{C}H_3$ of methyl ester group confirmed that PSIII is with very low DM or not methyl-esterified (Shakhmatov et al., 2016). From additional analysis of the COSY, TOCSY, ROESY and HMBC spectra, it was suggested that the carbon and proton resonances respectively at 183.3 ppm and 1.35-1.36 ppm arise from −CO and $-CH_3$ of fatty acids (RCOOH), which were detected in the initial linden PSC and probably partly left in PSIII after the alcohol pretreatment and anion-exchange chromatography of the linden PSin70 (not shown). A model structure of PSIII with some important H/H and C/H interactions from the NMR analyses are presented on Fig. 2.

3.1.4. FTIR analysis

The presence of acetyl esters is also confirmed by the FTIR study (Fig. S2), where bands with similar intensities at 1248 cm^{-1} ν(C—O—C)$_{Ac}$ and 1721 cm^{-1} ν(C═O)$_{Ac}$ are detected and disappear when the sample is saponified with NaOH (Paulsen, Fagerheim, & Øverbye, 1978). The bands at 3347 cm^{-1}, 2935 cm^{-1}, 1600 cm^{-1} and 1417 cm^{-1} for υ(OH), υ(CH), ν_{as}(COO$^-$) and ν_s(COO$^-$) are also observed (Filippov, Luknár, & Kohn, 1978). The presence of the signals at about 1151, 1037, 991, 958 and 819 cm^{-1} are also found in the linden PSC (Georgiev et al., 2017). Most of these signals, in addition to those at 916 and 844 cm^{-1} registered in the FTIR spectrum of PSIII are related to the RGI backbone structure according to the literature data (Kačuráková, Capek, Sasinková, Wellner, Ebringerová, 2000).

3.1.5. Small-angle X-ray scattering studies

In order to investigate the nanostructure of PSIII in water, SAXS experiments were performed. The absolute macroscopic scattering cross-section $d\Sigma/d\Omega(Q)$ as a function of modulus of the scattering vector Q ($Q = 4\pi \sin\left(\frac{\theta}{2}\right)/\lambda$, where λ = 1.54 Å and θ is the scattering angle) is depicted on Fig. 3. The function represents a typical polymer-like scattering at an intermediate and a high Q, while at a lower Q a significant upturn is observed with a close to Q^{-4} power-law characteristic for large clusters. This indicates the presence of larger aggregates (> 100 nm) in coexistence with chain-like molecules. Interestingly, the structure is essentially independent of concentration and temperature, suggesting rather long-lived stable aggregates. More quantitatively, the data can be described using a simple coexistence model of clusters and single chain (see section 2.8.). The fits provide an average molecular weight of 332 kDa for the dissolved chain, R_g = 4.6 nm and d_f = 1,7. The clusters are larger than what can be resolved by SAXS (> 100 nm) and could not be analyzed in details. The aggregation of pectins in aqueous solutions could be expected, thus different salts were used in the HPSEC and preparative SEC analyses to prevent it. Despite of the aggregation, the calculated M_w is in a good agreement with the determined values from HPSEC (382 kDa) and preparative SEC analyses (352 kDa).

3.2. Immunomodulating studies

We have already found that the linden PSC possesses *ex vivo* immunomodulating potential against human phagocytic leuko-

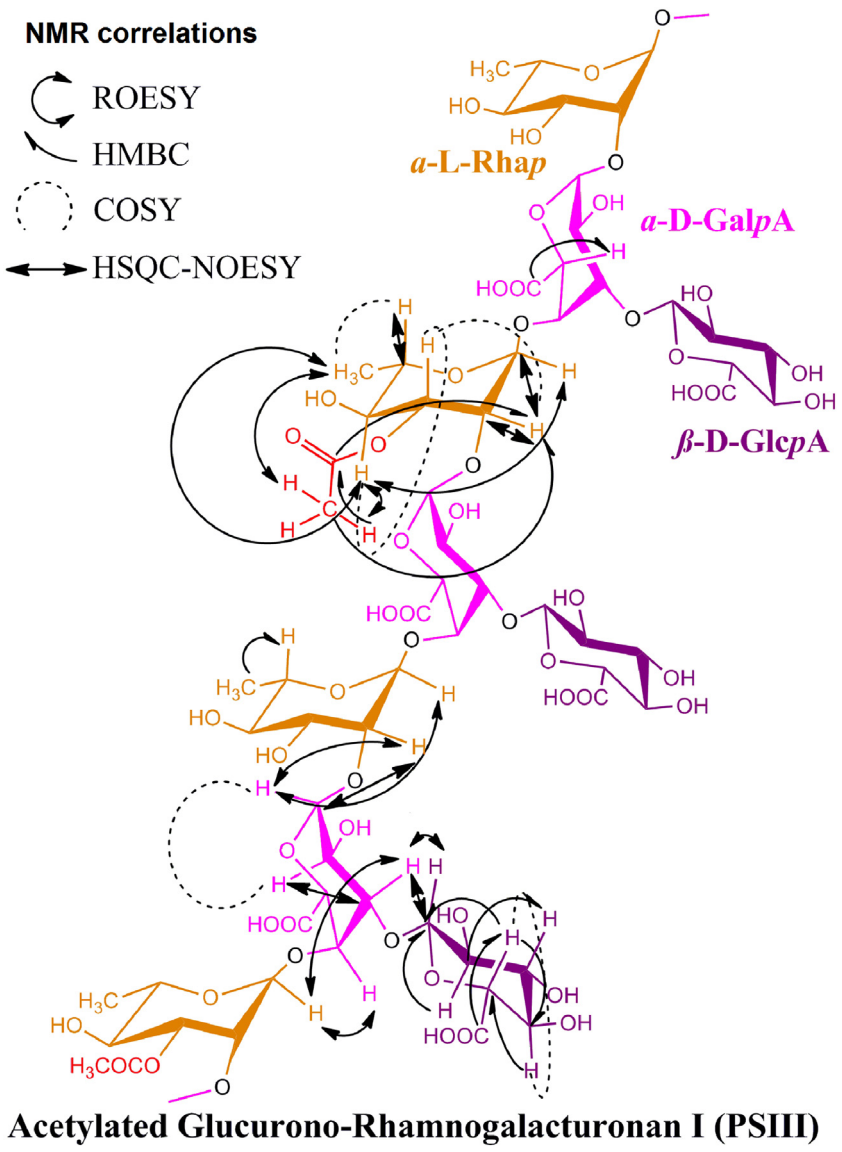


Fig. 2. Chemical structure of linden pectic fraction PSIII, elucidated by GC–MS glycosidic linkage analysis and 2D NMR spectroscopy. The most important H/H and C/H interactions are shown.

cytes, T-cells, murine PP cells and anti-tumor activity *in vitro* (Georgiev et al., 2017). In order to investigate the role of linden pectins in the observed immunomodulating activity of the initial linden PSC and to evaluate immune potency of each purified linden pectic fraction were performed some important biological experiments. In the following sections are presented the results from these experiments with purified linden pectic fractions.

3.2.1. Complement fixation activity

The three linden pectic fractions were tested against inhibition of human complement hemolysis of target SRBC *in vitro* (Fig. S3). PSI expressed the highest complement fixation activity with IC_{50} of 154.5 μg/ml, which was 4.7 fold higher than the IC_{50} value of the positive control, the highly active pectic polysaccharide BP-II from *B. petersianum* (Grønhaug et al., 2011). PSII and PSIII expressed lower activities, as IC_{50} value of PSIII was 491.6 μg/ml. Most probably the prevalence of the complement fixation activity of PSI was related to the presence of AGII structures active on the human complement system (Ho et al., 2016).

3.2.2. Phagocyte immune-response

3.2.2.1. Human WBP and isolated neutrophils

The typical pectic polysaccharide (PSI) and the two GlcA-RGsI (PSII and PSIII) increased ROS production from WBP at 100 μg/ml and only PSIII increased CL response from isolated neutrophils (Fig. 4A and B). Meanwhile, with co-stimulation by PMA, PSI and PSIII did not increase the ROS production from WBP, however PSII slightly enhanced the ROS formation at a concentration of 100 μg/ml (Fig. 4A). Interestingly, under the condition on a co-stimulation with OZP, PSI and PSII clearly decreased the ROS production at the higher concentration of 100 μg/ml in comparison with the control of the OZP stimulation alone (Fig. 4A). However, all polysaccharide fractions did not show a clear enhancing activity on the ROS formation from the isolated neutrophils in the presence of PMA and OZP (Fig. 4B). PMA and OZP significantly increased the CL signal of both WBP and isolated neutrophils. In the case of spontaneous ROS formation the CL signal caused by the linden pectins at the higher concentration of 100 μg/ml was much lower than those

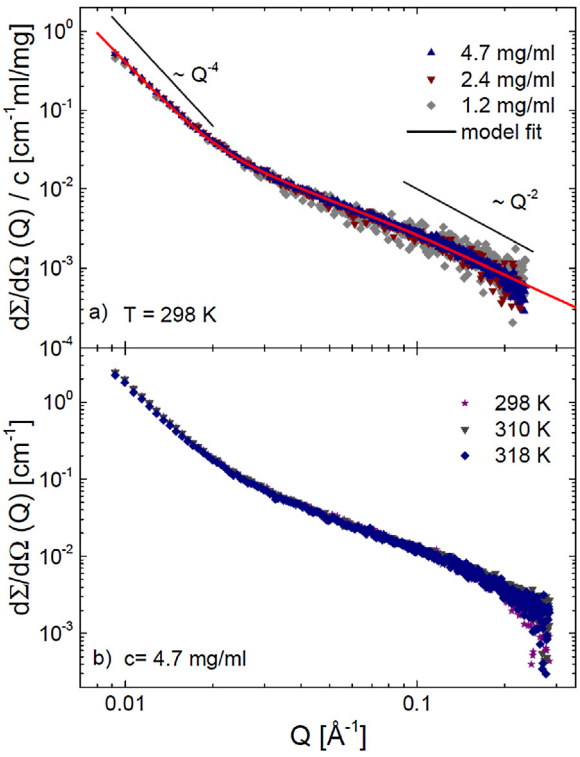


Fig. 3. Small-angle X-ray scattering data showing the absolute macroscopic scattering cross-section $d\Sigma/d\Omega(Q)$ as a function of modulus of the scattering vector, Q for PSIII aqueous solutions. a) at different concentrations and b) at different temperatures.

in the presence of PMA or OZP (Fig. 4A and B). When the effect of the polysaccharide fractions on the expression of CD18 and CD62L on isolated neutrophils was analyzed, only PSIII showed a weak effect on CD18 expression (Fig. S4). This was in agreement with the results from the spontaneous ROS production from both WBP and isolated neutrophils. It was proposed that the unique glucuronidated RGI structure of PSIII might be involved in the observed effects.

3.2.2.2. *Murine macrophages*

Macrophage activation can be evaluated by the release of antimicrobial NO under the catalytic action of iNOS. The purified linden pectins did not have a cytotoxic effect on the RAW 264.7 cells on the basis of the LDH test (Fig. S5). When the iNOS induction was analyzed by western blotting, the stimulation with all linden pectic fractions for 24 h increased the iNOS protein level of the RAW 264.7 cells. The co-stimulation with LPS (10 ng/ml) in the presence of the polysaccharides significantly enhanced the iNOS protein level by comparison with the stimulating condition with the purified pectins alone (Fig. 5A). Otherwise, the simultaneous treatment of the macrophages with LPS and linden polysaccharides led to statistically significant lower iNOS levels at 100 μg/ml than at 50 μg/ml for PSI and PSIII. This effect was similar to the reduction of the ROS formation from WBP co-stimulated with OZP and PSI or PSII (Fig. 4A). When the RAW 264.7 cells were stimulated with the linden pectic fractions for 48 h, the iNOS production reached almost to the same level as that observed in the co-stimulation condition with LPS and linden fractions (Fig. 5A). Similarly to the results from 24 h, the iNOS levels in the cells co-treated with LPS and PSI or PSIII at 100 μg/ml after 48 h were slightly decreased in comparison with the pectic fractions alone. But unlike the results from 24 h, where there was not observed any clear difference in the iNOS expression induced by three samples alone, after 48 h PSI exhibited a higher induction activity at the both studied concentrations.

Meanwhile, the stimulation effect of polysaccharide fractions, alone or in a combination with LPS was analyzed on the NO production from RAW 264.7 cells (Fig. 5B). The NO production was dramatically increased by the stimulation with all fractions for 24 h at concentrations of 50 and 100 μg/ml compared with the growth medium control. The NO release in the control medium was negligible, therefore the adherent cells were not activated by the plate surface. The stimulating activity of PSII seemed to be weaker than those of PSI and PSIII, and there was no a significant difference between the stimulatory activities of PSI and PSIII. However, the combinatorial effect of linden polysaccharides with LPS was tested, and the NO production induced by all linden pectins at 100 μg/ml were lower in comparison with the production in the stimulation with the polysaccharide fractions alone (Fig. 5B). When the stimulation was prolonged for 48 h, PSI induced more than 2 fold higher NO production than PSIII, which could be explained by the different structural features of both samples ($p < 0.001$). This result was in agreement with the iNOS expression after 48 h of incubation (Fig. 5A). After 48 h NO production in the co-stimulation condition was reduced again at 100 μg/ml in comparison with the separate polysaccharide treatments ($p < 0.001$) (Fig. 5B). This effect was in agreement with the iNOS expression levels after 24 h and 48 h of macrophage stimulation. From the cytotoxicity data, combinations with LPS showed relative absorbance units close to the control, which was another confirmation for the suppression-like effect on the LPS-induced inflammatory response in macrophages (Fig. S5). For elucidation of this phenomenon more studies on the effect of linden polysaccharides on the iNOS expression with higher doses are needed.

3.2.3. *Intestinal immunomodulating activity*

It has been found that the linden PSC exhibited *ex vivo* intestinal immunomodulating activity through the PP-mediated bone mar-

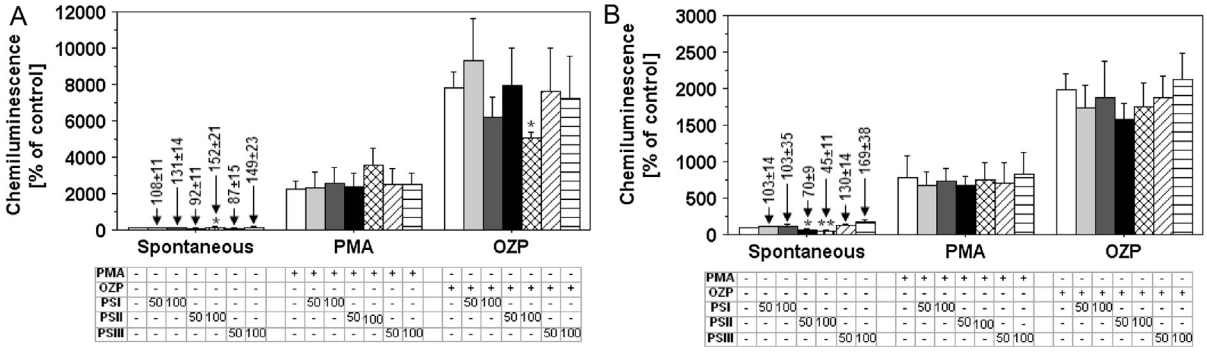


Fig. 4. Effect of linden pectic fractions (PSI-PSIII) on A) ROS production from non-stimulated (spontaneous), PMA- and OZP-activated human whole blood phagocytes. B) ROS production from isolated neutrophils. 50 (50 μg/ml) and 100 (100 μg/ml). The asterisks indicate statistical significance (*$p < 0.05$, **$p < 0.01$) vs. control.

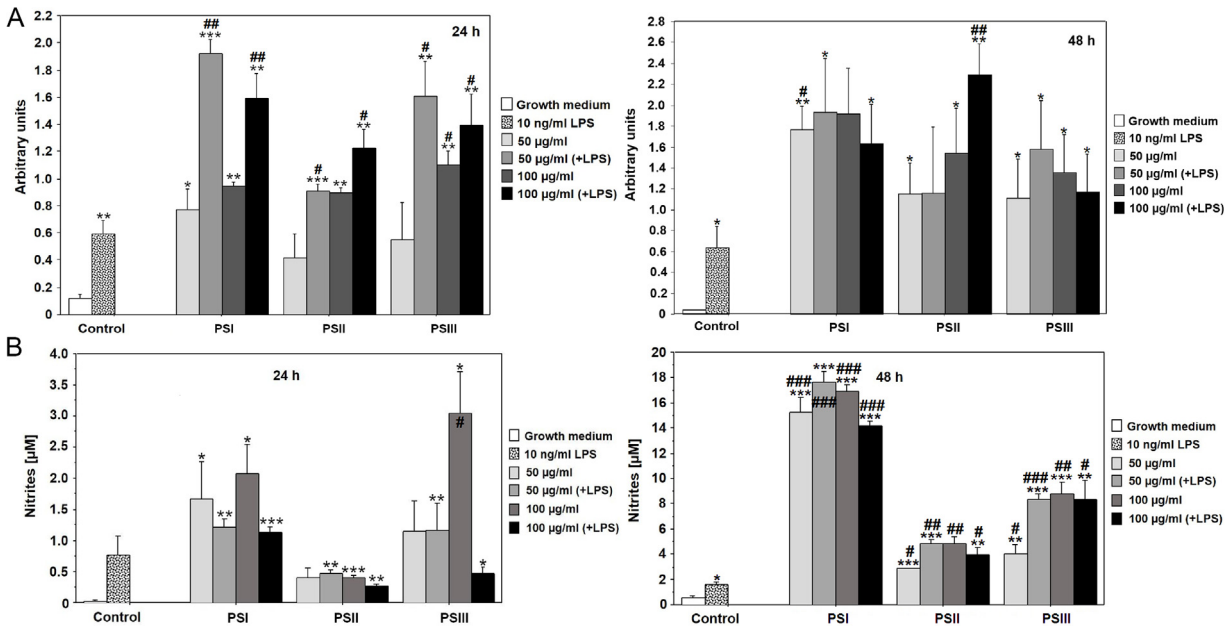


Fig. 5. Effect of linden pectic fractions on A) iNOS expression in RAW 264.7 cells cultured with samples alone or co-stimulated with LPS. B) NO production from RAW 264.7 cells cultured with samples alone or co-stimulated with LPS. LPS from *E. coli* was used as a positive control. The asterisks indicate statistical significance (*$p < 0.05$, **$p < 0.01$, ***$p < 0.001$) vs. control – growth medium (untreated cells) and (#$p < 0.05$, ##$p < 0.01$, ###$p < 0.001$) vs. LPS.

row cell proliferation test and increased IL-6 production from the PP cells (Georgiev et al., 2017). In order to clarify whether partially purified polysaccharides (PSI-PSIII) also show activity, their stimulatory potential was investigated as well. However, only PSI expressed a weak activity ($p < 0.01$) and PSII and PSIII were inactive (Fig. S6).

3.2.4. Anti-tumor activity

When we found that the linden pectins exhibited immunomodulating properties against phagocytes, we decided to test their effect on abnormal cells. In a previous study, the linden PSC expressed a non-specific inhibitory activity against different tumor cell lines and normal amniotic cells and fibroblasts *in vitro* (Georgiev et al., 2017). On the basis of our preliminarily screening results with PSI and PSIII, we found that in addition to the tumor cells, polysaccharides inhibited in a similar degree the growth of the studied FL cells (Fig. S7).

4. Discussion

The need of a further characterization of the silver linden pectins was provoked by elucidation of the role of different pectic fractions as immunomodulating compounds in *Tilia* flowers and also due to the traditional use of the linden tea and mucilage. It was found that PSI is a low-esterified typical pectic polysaccharide with HG and RGI, which is O-4 substituted at the Rha units with 1,3,5-arabinans and highly branched bioactive AGII structures. Furthermore, it was suggested that PSI contains trace amounts of RGII on the basis of the KDO test, the presence of 1,3,4-linked GalA residues and the trace amounts of Fuc. PSII and PSIII are two unusual high molecular weight free RGI polymers that are highly acetylated and highly glucuronidated, almost lacking neutral sugar side chains. Renard et al. (1999) estimated that one GalA unit out of 72 are O-3 substituted with GlcA in sugar beet RGI. Sengkhamparn et al. (2009) found for the first time that Rha in okra pectic RGI can be O-3 acetylated. Later, Leijdekkers, Huang, Bakx, Gruppen, and Schols (2015) reported that a single GalA unit in the RGI from sugar beet pectin could be both acetylated and substituted with GlcA. In the present study it was demonstrated that silver linden flowers contain a unique RGI (PSIII) in which almost every GalA unit is O-3 glucuronidated and at the same time significantly acetylated (>30%) at O-3 of the Rha residues. The O-3 glucuronidated RGI core structure was found in the mucilage of the inner bark of *Hydrangea paniculata* Sieb. in 1976–1977 (Tomoda & Satoh, 1977). The structure is not found often in plants and to our knowledge, it has not been isolated from flowering plant organs (Shimizu & Tomoda, 1985).

Phagocytic leukocytes, such as macrophages and neutrophils, producing ROS and NO play a key role in the innate immunity. They are also involved in the acute inflammatory diseases, thus a proper modulation of their activation is often needed. Our findings suggest that the three purified polysaccharide fractions (PSI-PSIII) are active ingredients in the crude linden PSC for enhancing activity on the ROS production of human WBP and neutrophils (Georgiev et al., 2017). Prevalence in the activity was observed for PSII and PSIII, as only PSIII increased the ROS production from isolated neutrophils. It was suggested that the unique glucuronidated RGI structure of PSIII was important for expression of the activity, which was supported by the weak increase of the surface β_2-integrin levels on neutrophils induced by the sample (Fig. S4). However, the effect of the three polysaccharides was negligible in comparison with the potent activators PMA, OZP and fMLP (Figs. 4 & S4). Furthermore, the effect of PSI-III against the spontaneous ROS generation from WBP at 100 μg/ml was lower than this for the crude linden PSC (420 ± 60%), which could be explained by the combinatorial action of different active compounds in the complex (Georgiev et al., 2017). On the other hand, PSI and PSIII expressed a suppression-like activity on the OZP-induced activation of WBP at the higher concentration of 100 μg/ml, which was not observed with the linden PSC (Georgiev et al., 2017). This effect was also not observed in the experiments with isolated neutrophils. Kiyohara, Matsumoto, Nagai, Kim, & Yamada (2006) showed a significant positive correlation between the reactivity of pectic polysaccharides with IgG and the degree of complement-activating ability. PSI expressed a high complement fixation activity, which supposed that the linden polysaccharides could interact with some blood serum components like antibodies and then act in such a manner to negatively influence the OZP-initiated oxidative burst. Interestingly, Popov, Ovodova, Popova, Nikitina, and Ovodov (2005) reported that a pectic polysaccharide

(100 μg/ml) from *Comarum palustre* does not influence the OZP-activated ROS generation from human neutrophils, but it could reduce the PMA-induced ROS production. The crude linden PSC also enhanced the spontaneous ROS production from WBP and did not increase the CL signal under the co-stimulation with PMA (Georgiev et al., 2017). The three pectic fractions did not contribute to a synergistic increase of the ROS production from the PMA- and OZP-treated neutrophils.

The induction of NO production by the linden pectins did not lead to severe cytotoxic effects under the studied conditions (Fig. S5). PSI expressed a higher macrophage stimulating activity than PSII and PSIII, as probably the RGI AG side chains are important for the macrophage activation, as described in the literature (Grønhaug et al., 2010). Generally, our results from the NO production demonstrated that linden pectins could activate macrophages and this was in agreement with the increased human $CD14^+$ and $CD64^+$ white blood cells and induction of IL-6 production by the linden PSC (Georgiev et al., 2017). The linden pectins exhibited suppression-like effect on the LPS-induced inflammatory response in macrophages, shown by reduction of the iNOS expression and NO production. However, both LPS and linden polysaccharides alone were inductors of the iNOS and NO production. Therefore, there was not a synergism between the microbial antigen and the plant antigen-mimetic, as was expected and even observed by Zhu et al. (2012) for a combination between LPS and a polysaccharide from *Chaenomeles speciosa* fruit. The observed effect suggests that the linden pectins have a potential for stimulation of the innate immunity and suppression of the LPS-induced macrophage inflammatory process similarly to the reduction of the OZP-induced ROS generation from WBP. This could be explained by the proposed polysaccharide anti-inflammatory behavior, which could be useful in supplementation during treatment of autoimmune and infectious diseases. In fact, *T. tomentosa* is famous with its anti-inflammatory action which is attributed mainly to its flavonoids, but probably polysaccharides also contribute to this effect (Allio et al., 2015; Matsuda et al., 2002; Viola et al., 1994). Similar to the dual effect observed in our study was also reported for fucoidan, which stimulated the NO release from RAW 264.7 cells at 100 μg/ml alone, but in a combination with LPS at concentrations higher than 10 μg/ml it inhibited the LPS-stimulated NO release and iNOS expression (Nakamura, Suzuki, Wada, Kodama, & Doi, 2006; Yang, Yoon, Oh, Kim, & Kang, 2006). Authors concluded that the fucoidan may not act on the extracellular receptors, but on the intracellular signaling machinery, such as the process of transcription factor activation. Chen et al. (2006) reported that the LPS-induced (100 ng/ml) iNOS expression level in RAW 264.7 cells was similar to those obtained by a co-stimulation with LPS and DE90 citrus pectin, but increasing of the pectin concentration resulted in a decrement of the iNOS protein expression. They found that DE90 pectin had a potential to inhibit the downstream signals of LPS, and proposed that the inhibition was not a result of the DE90 directly inhibiting the activities of signal proteins, but from the pectin-LPS interactions or different affinity to cell-surface receptors.

The role of GlcA in plant polysaccharides and its impact on the biological activity are intriguing but still not fully elucidated (Grønhaug et al., 2011; Kiyohara et al., 2010). Interestingly, Duan, Chen, Dong, Ding, and Fang (2010) showed that pectin from *D. kaki* structurally similar to PSIII could inhibit the LPS-induced B-cell proliferation and had no effect on the Concanavalin A-induced T-cell proliferation. This, together with our results also suggests that GlcA might be involved in the suppression effect of the linden pectins on the LPS-induced and OZP-induced inflammatory response in macrophages and WBP.

Normally, herbal polysaccharides are contained in infusions, extracts, traditional foods and are administered orally from these formulations. Pectins are little absorbed by the intestinal epithelium, but they may interact with the mucosal immune system through immunocompetent cells in the PP localized in the small intestine. By this mode of action of the active polysaccharides, functionally modulated immunocompetent cells are proposed to result in modulations of several mucosal and systemic immune systems (Yamada & Kiyohara, 2007). Only PSI showed a weak activity ($p < 0.01$) probably related to RGI AG side chains as found previously (Grønhaug et al., 2011; Kiyohara et al., 2010). Maybe acetylated RGI backbone and attached GlcA in PSIII were not enough for expression of activity.

The neutrophils and macrophages are involved in the regulation of both innate and adaptive immunity in various inflammatory processes including tumor diseases. The phagocytes present in the tumor microenvironment can promote or inhibit cancer formation and development (Mantovani, 2014). Brizi et al. (2012) reported that aqueous and ethanol extracts from the flowers of *Tilia x viridis* (*T. tomentosa* and *T. americana* hybrid) exhibited anti-proliferative effects on BW 5147 cells (T-cell lymphoma) and normal Concanavalin A-stimulated lymphocytes *in vitro*, as they related the activity to polyphenols. Our preliminarily screening study with the MTT test demonstrated that linden pectins expressed a non-selective growth inhibitory activity against tumor cells and the studied normal FL cells (Fig. S7). However, PSI-PSIII did not show cytotoxic effects (LDH test) on murine macrophages (Fig. S5) and they did not inhibit the proliferation of murine PP immunocompetent cells (Fig. S6). The difference between the polysaccharide effect on the FL cells and the studied immune cells could be explained primarily by their different functions in the organism. Generally, the immune cells could be activated by complex pectins unlike the tumor cells and probably FL cells.

5. Conclusions

In the current paper, we show that the silver linden blossoms contain two structurally different pectic type polysaccharides – a low-esterified typical pectic polysaccharide PSI (M_w = 28.2 kDa) and unusual considerably acetylated (2.9-3.3%) and glucuronidated RGI polymers PSII (M_w = 949 kDa) and PSIII (M_w = 382 kDa). Furthermore, PSIII is a unique RGI macromolecule, which GalA residues are almost completely O-3 glucuronidated and >30% acetylated at O-3 of the Rha units. The three pectic fractions could stimulate the innate immune response through induction of the ROS and NO generation by neutrophils and macrophages in a non-aggressive manner. At the same time, silver linden pectins suppressed the OZP-activated ROS generation and the LPS-induced iNOS expression and NO production by WBP and murine macrophages, respectively. This dual mode of action on the phagocytes revealed the anti-inflammatory potential of the silver linden polysaccharides. Furthermore, PSI showed the highest complement fixation (IC_{50} = 154.5 μg/ml) and macrophage stimulating (almost 18 μM NO production after 48 h) activities and at the same time, it was the only sample expressing intestinal immunomodulating activity against PP cells. It was shown for the first time that acetylated and highly glucuronidated RGI may exhibit immunomodulating properties via neutrophil and macrophage activation, and suppression of viability of different tumor cell lines. On the basis of our results, we conclude that pectins in *T. tomentosa* inflorescences are immune-active compounds. The silver linden pectins deserve to be included in the supplementary therapy research for prevention and treatment of immune related diseases like inflammatory diseases.

Acknowledgements

We would like to thank Dr. Mariana Nikolova (Plovdiv University Paisii Hilendarski) for kindly providing the herbal material.

We are also indebted to Dr. Veronika Sivova for performing the complement assay. This work was supported by the European Regional Development Fund, EU [Grant № BG161PO0003-1.1.05-0024-C0001, 2012-2014], European Social Fund, EU [Grant no BG051PO001/3.3-05-0001, 2014], the Ministry of Education, Youth and Sport of the Czech Republic [Grant no LQ1605 NPU II; project MSM0021622430], Erasmus+ Programme and EEA grants. The Research Council of Norway is acknowledged for financial support through the Norwegian NMR Platform, NNP (226244/F50).

Appendix A. Supplementary data

Supplementary data associated with this article can be found, in the online version, at http://dx.doi.org/10.1016/j.carbpol.2017.07.073.

References

Allio, A., Calorio, C., Franchino, C., Gavello, D., Carbone, E., & Marcantoni, A. (2015). Bud extracts from *Tilia tomentosa* Moench inhibit hippocampal neuronal firing through GABAA and benzodiazepine receptors activation. *Journal of Ethnopharmacology*, *172*, 288–296.

Anthon, G. E., & Barrett, D. M. (2008). Combined enzymatic and colorimetric method for determining the uronic acid and methyl ester content of pectin: Application to tomato products. *Food Chemistry*, *110*, 239–247.

Arcos, M. L. B., Cremaschi, G., Werner, S., Coussio, J., Ferraro, G., & Anesini, C. (2006). *Tilia cordata* Mill. extracts and scopoletin (isolated compound): Differential cell growth effects on lymphocytes. *Phytotherapy Research*, *20*(1), 34–40.

Barsett, H., Paulsen, B. S., & Habte, Y. (1992). Further characterization of polysaccharides in seeds from *Ulmus glabra* Huds. *Carbohydrate Polymers*, *18*(2), 125–130.

Beaucage, G. (1996). Small-angle scattering from polymeric mass fractals of arbitrary mass-fractal dimension. *Journal of Applied Crystallography*, *29*, 134–146.

Bijak, M., Saluk, J., Tsirigotis-Maniecka, M., Komorowska, H., Wachowicz, B., Zaczyńska, E., et al. (2013). The influence of conjugates isolated from *Matricaria chamomila* L. on platelets activity and cytotoxicity. *International Journal of Biological Macromolecules*, *61*, 218–229.

Blumenkrantz, N., & Asboe-Hansen, G. (1973). New method for quantitative determination of uronic acids. *Analytical Biochemistry*, *54*, 484–489.

Bradford, M. M. (1976). A rapid and sensitive method for the quantification of microgram quantities of protein utilizing the principle of protein-dye binding. *Analytical Biochemistry*, *72*, 248–254.

Brizi, M. R., Marrassini, C., Zettler, G., Ferraro, G., & Anesini, C. (2012). Comparative antiproliferative action of two extracts from *Tilia* × *viridis* on normal and tumoral lymphocytes: Relationship with antioxidant activity. *Chinese Medicine*, *3*, 20–29.

Chambers, R. E., & Clamp, J. R. (1971). An assessment of methanolysis and other factors used in the analysis of carbohydrate-containing materials. *Biochemical Journal*, *125*, 1009–1018.

Chen, C. H., Sheu, M. T., Chen, T. F., Wang, Y. C., Hou, W. C., Liu, D. Z., et al. (2006). Suppression of endotoxin-induced proinflammatory responses by citrus pectin through blocking LPS signaling pathways. *Biochemical Pharmacology*, *72*(8), 1001–1009.

Chinou, I. (2012a). *Assessment report on Tilia cordata Miller, Tilia platyphyllos Scop., Tilia x vulgaris Heyne or their mixtures, flos*. European Medicines Agency, Committee on Herbal Medicinal Products., 337067/2011

Chinou, I. (2012b). *Assessment report on Tilia tomentosa Moench, flos*. European Medicines Agency, Committee on Herbal Medicinal Products., 346780/2011.

Ciucanu, I., & Kerek, F. (1984). A simple and rapid method for the permethylation of carbohydrates. *Carbohydrate Research*, *131*(2), 209–217.

de Santana-Filho, A. P., Noleto, G. R., Gorin, P. A. J., de Souza, L. M., Iacomini, M., & Sassaki, G. L. (2012). GC–MS detection and quantification of lipopolysaccharides in polysaccharides through 3-O-acetyl fatty acid methyl esters. *Carbohydrate Polymers*, *87*, 2730–2734.

Denman, L. J., & Morris, G. (2015). An experimental design approach to the chemical characterisation of pectin polysaccharides extracted from *Cucumis melo* Inodorus. *Carbohydrate Polymers*, *117*, 364–369.

Duan, J., Chen, V. L., Dong, Q., Ding, K., & Fang, J. (2010). Chemical structure and immunoinhibitory activity of a pectic polysaccharide containing glucuronic acid from the leaves of *Diospyros kaki*. *International Journal of Biological Macromolecules*, *46*, 465–470.

Dubois, M., Gilles, K. A., Hamilton, J. K., Rebers, A., & Smith, F. (1956). Colorimetric method for determination of sugars and related substances. *Analytical Chemistry*, *28*(3), 350–356.

Fan, Y., Sun, C., Gao, X., Wang, F., Li, X., Kassim, R. M., et al. (2012). Neuroprotective effects of ginseng pectin through the activation of ERK/MAPK and Akt survival signaling pathways. *Molecular Medicine Reports*, *5*(5), 1185–1190.

Filippov, M. P., Luknár, O., & Kohn, R. (1978). Infrared spectra of the acetyl derivatives of pectin. I. Potassium salts of the citrus pectic acid with different degrees of acetylation. *Chemical Papers*, *32*(2), 211–217.

Gallova, L., Kubala, L., Ciz, M., & Lojek, A. (2004). IL-10 does not affect oxidative burst and expression of selected surface antigen on human blood phagocytes *in vitro*. *Physiological Research*, *53*, 199–208.

Georgiev, Y., Ognyanov, M., Yanakieva, Y., Kussovski, V., & Kratchanova, M. (2012). Isolation, characterization and modification of citrus pectin. *Journal of BioScience and Biotechnology*, *1*, 223–233.

Georgiev, Y. N., Ognyanov, M. H., Kiyohara, H., Batsalova, T. G., Dzhambazov, B. M., Ciz, M., et al. (2017). Acidic polysaccharide complexes from purslane, silver linden and lavender stimulate Peyer's patch immune cells through innate and adaptive mechanisms. *International Journal of Biological Macromolecules*, http://dx.doi.org/10.1016/j.ijbiomac.2017.07.095

Grønhaug, T. E., Ghildyal, P., Barsett, H., Michaelsen, T. E., Morris, G., Diallo, D., et al. (2010). Bioactive arabinogalactan from the leaves of *Opilia celtidifolia* Endl. ex Walp. (Opiliaceae). *Glycobiology*, *20*(12), 1654–1664.

Grønhaug, T. E., Kiyohara, H., Sveaass, A., Diallo, D., Yamada, H., & Paulsen, B. S. (2011). Beta-D-(1 → 4)-galactan-containing side chains in RG-I regions of pectic polysaccharides from *Biophytum petersianum* Klotzsch. contribute to expression of immunomodulating activity against intestinal Peyer's patch cells and macrophages. *Phytochemistry*, *72*, 2139–2147.

Groudeva, J., Kratchanova, M. G., Panchev, I. N., & Kratchanov, C. G. (1997). Application of granulated apple pectin in the treatment of hyperlipoproteinaemia. *Zeitschrift für Lebensmittel-Untersuchung und –Forschung*, *204*, 374–378.

Ho, G. T. T., Zou, Y.-F., Aslaksen, T. H., Wangensteen, H., & Barsett, H. (2016). Structural characterization of bioactive pectic polysaccharides from elderflowers (*Sambuci flos*). *Carbohydrate Polymers*, *135*, 128–137.

Holderness, J., Schepetkin, I. A., Freedman, B., Kirpotina, L. N., Quinn, M. T., Hedges, J. F., et al. (2011). Polysaccharides isolated from açaí fruit induce innate immune responses. *PLOS ONE*, *6*(2), e17301.

Hong, T., Matsumoto, T., Kiyohara, H., & Yamada, H. (1998). Enhanced production of hematopoietic growth factors through T-cell activation in Peyer's patches by oral administration of Kampo (Japanese herbal) medicine, Juzen-Taiho-To. *Phytomedicine*, *5*, 353–360.

Hritcu, L., & Cioanca, O. (2016). Prevalence of use of herbal medicines and complementary and alternative medicine in Europe. In C. Grosso (Ed.), *Herbal medicine in depression* (pp. 135–182). Switzerland: Springer International Publishing.

Inngjerdingen, K. T., Kiyohara, H., Matsumoto, T., Petersen, D., Michaelsen, T. E., Diallo, D., et al. (2007). An immunomodulating pectic polymer from *Glinus oppositifolius*. *Phytochemistry*, *68*, 1046–1058.

Inngjerdingen, M., Inngjerdingen, K. T., Patel, T. R., Allen, S., Chen, X., Rolstad, B., et al. (2008). Pectic polysaccharides from *Biophytum petersianum* Klotzsch, and their activation of macrophages and dendritic cells. *Glycobiology*, *18*(12), 1074–1084.

Kačuráková, M., Capek, P., Sasinková, V., Wellner, N., & Ebringerová, E. (2000). FT-IR study of plant cell wall model compounds: Pectic polysaccharides and hemicelluloses. *Carbohydrate Polymers*, *43*, 195–203.

Kim, J., & Carpita, N. C. (1992). Changes in esterification of the uronic acid groups of cell wall polysaccharides during elongation of maize coleoptiles. *Plant Physiology*, *98*(2), 646–653.

Kiyohara, H., Matsumoto, T., Nagai, T., Kim, J.-S., & Yamada, H. (2006). The presence of natural human antibodies reactive against pharmacologically active pectic polysaccharides from herbal medicines. *Phytomedicine*, *13*, 494–500.

Kiyohara, H., Uchida, T., Takakiwa, M., Matsuzaki, T., Hada, N., Takeda, T., et al. (2010). Different contributions of side-chains in *β*-D-(1 → 3, 6)-galactans on intestinal Peyer's patch-immunomodulation by polysaccharides from *Astragalus mongholics* Bunge. *Phytochemistry*, *71*, 280–293.

Kosakowska, O. K., Bączeka, K., Przybył, J. L., Ejdys, M., Kuźma, P., Obiedziński, M., et al. (2015). Intraspecific variability in the content of phenolic compounds, essential oil and mucilage of small-leaved lime (*Tilia cordata* Mill.) from Poland. *Industrial Crops and Products*, *78*, 58–65.

Kram, G., & Franz, G. (1983). Untersuchungen über die Schleimpolysaccharide aus Lindenblüten. *Planta Medica*, *49*, 149–153.

Kram, G., & Franz, G. (1985). Structural investigations on the watersoluble polysaccharides of lime tree flowers (*Tilia cordata* L.). *Pharmazie*, *40*, 501–502.

Leijdekkers, A. G. M., Huang, J.-H., Bakx, E. J., Gruppen, H., & Schols, H. A. (2015). Identification of novel isomeric pectic oligosaccharides using hydrophilic interaction chromatography coupled to travelling-wave ion mobility mass spectrometry. *Carbohydrate Research*, *404*, 1–8.

Liu, Y., Dong, M., Yang, Z., & Pan, S. (2016). Anti-diabetic effect of citrus pectin in diabetic rats and potential mechanism via PI3K/Akt signaling pathway. *International Journal of Biological Macromolecules*, *89*, 484–488.

Lojek, A., Ciz, M., Pekarova, M., Ambrozova, G., Vasicek, O., Moravcova, J., et al. (2011). Modulation of metabolic activity of phagocytes by antihistamines. *Interdisciplinary Toxicology*, *4*(1), 15–19.

Ma, L., Qin, C., Wang, M., Gan, D., Cao, L., Ye, H., et al. (2013). Preparation, preliminary characterization and inhibitory effect on human colon cancer HT-29 cells of an acidic polysaccharide fraction from *Stachys floridana* Schuttl. ex Benth. *Food and Chemical Toxicology*, *60*, 269–276.

McComb, E. A., & McCready, R. M. (1957). Determination of acetyl in pectin and in acetylated carbohydrate polymers (Hydroxamic acid reaction). *Analytical Chemistry*, *29*, 819–821.

Mantovani, A. (2014). Macrophages, neutrophils, and cancer: A double edged sword. *New Journal of Science*, 271940 http://dx.doi.org/10.1155/2014/271940

Manuele, M. G., Ferraro, G., & Anesini, C. (2008). Effect of *Tilia* × *viridis* flower extract on the proliferation of a lymphoma cell line and on normal murine lymphocytes: Contribution of monoterpenes, especially limonene. *Phytotherapy Research*, *22*(11), 1520–1526.

Matsuda, H., Ninomiya, K., Shimoda, H., & Yoshikawa, M. (2002). Hepatoprotective principles from the flowers of *Tilia argentea* (Linden): Structure requirements of tiliroside and mechanisms of action. *Bioorganic and Medicinal Chemistry*, *10*, 707–712.

McNeil, M., Darvill, A. G., & Albersheim, P. (1980). X. Rhamnogalacturonan I, a structurally complex pectic polysaccharide in the cell walls of suspension-cultured sycamore cells. *Plant Physiology*, *66*, 1128–1134.

Michaelsen, T. E., Gilje, A., Samuelsen, A. B., Høåsen, K., & Paulsen, B. S. (2000). Interaction between human complement and a pectin type polysaccharide fraction, PMII, from the leaves of *Plantago major* L. *Scandinavian Journal of Immunology*, *52*, 483–490.

Nakamura, T., Suzuki, H., Wada, Y., Kodama, T., & Doi, T. (2006). Fucoidan induces nitric oxide production via p38 mitogen-activated protein kinase and NF-kB-dependent signaling pathways through macrophage scavenger receptors. *Biochemical and Biophysical Research Communications*, *343*(1), 286–294.

Nauseef, W. M. (2014). Isolation of human neutrophils from venous blood. In M. T. Quinn, & F. R. DeLeo (Eds.), *Methods in molecular biology 1124, Neutrophil methods and protocols* (pp. 13–18). New York: Humana Press Inc.

Ohtani, K., Okai, K., Yamashita, U., Yuasa, I., & Misaki, A. (1995). Characterization of an acidic polysaccharide isolated from the leaves of *Corchorus olitorius* (Moroheiya). *Bioscience, Biotechnology, and Biochemistry*, *59*(3), 378–381.

Paulsen, B. S., & Barsett, H. (2005). Bioactive pectic polysaccharides. In T. Heinze (Ed.), *Advances in polymer science 186, polysaccharides I. structure, characterization and use* (pp. 69–101). Berlin Heidelberg: Springer-Verlag.

Paulsen, B. S., Fagerheim, E., & Øverbye, E. (1978). Structural studies of the polysaccharide from *Aloe plicatilis* Miller. *Carbohydrate Research*, *60*, 345–351.

Pekarova, M., Lojek, A., Martiskova, H., Vasicek, O., Bino, L., Klinke, A., et al. (2011). New role for L-arginine in regulation of inducible nitric-oxide-synthase-derived superoxide anion production in Raw 264.7 macrophages. *The Scientific World Journal*, *11*, 2443–2457.

Popov, S. V., Ovodova, R. G., Popova, G. Y., Nikitina, I. R., & Ovodov, Y. S. (2005). Adhesion of human neutrophils to fibronectin is inhibited by comaruman, pectin of marsh cinquefoil *Comarum palustre* L., and by its fragments. *Biochemistry (Moscow)*, *70*(1), 133–138.

Radoglou, K., Dobrowolska, D., Spyroglou, G., & Nicolescu, V.-N. (2009). A review on the ecology and silviculture of limes (*Tilia cordata* Mill., *Tilia platyphyllos* Scop. and *Tilia tomentosa* Moench.) in Europe. *Die Bodenkultur*, *60*(3), 9–19.

Ravenscroft, N., Cescutti, P., Gavini, M., Stefanetti, G., MacLennan, C. A., Martin, L. B., et al. (2015). Structural analysis of the O-acetylated O-polysaccharide isolated from *Salmonella paratyphi* A and used for vaccine preparation. *Carbohydrate Research*, *404*, 108–116.

Renard, C. M. G. C., & Jarvis, M. C. (1999). Acetylation and methylation of homogalacturonans 1: Optimization of the reaction and characterization of the products. *Carbohydrate Polymers*, *39*, 201–207.

Renard, C. M. G. C., Crépeau, M.-J., & Thibault, J.-F. (1999). Glucuronic acid directly linked to galacturonic acid in the rhamnogalacturonan backbone of beet pectins. *European Journal of Biochemistry*, *266*, 566–574.

Ridley, B. L., O'Neill, M. A., & Mohnen, D. (2001). Pectins: Structure, biosynthesis, and oligogalacturonide-related signaling. *Phytochemistry*, *57*, 929–967.

Schmidgall, J., Schnetz, E., & Hensel, A. (2000). Evidence for bioadhesive effects of polysaccharides and polysaccharide-containing herbs in an *ex vivo* bioadhesion assay on buccal membranes. *Planta Medica*, *66*, 48–53.

Schols, H. A., & Voragen, A. G. J. (2002). The chemical structure of pectins. In G. B. Seymour, & J. P. Knox (Eds.), *Pectins and their manipulation* (pp. 1–29). Oxford: Blackwell Publishing, CRC Press.

Sengkhamparn, N., Bakx, E. J., Verhoef, R., Schols, H. A., Sajjaanantakul, T., & Voragen, A. G. J. (2009). Okra pectin contains an unusual substituion of its rhamnosyl residues with acetyl and alpha-linked galactosyl groups. *Carbohydrate Research*, *344*, 1842–1851.

Shakhmatov, E. G., Udoratina, E. V., Atukmaev, K. V., & Makarova, E. N. (2015). Extraction and structural characteristics of pectic polysaccharides from *Abies sibirica* L. *Carbohydrate Polymers*, *123*, 228–236.

Shakhmatov, E. G., Atukmaev, K. V., & Makarova, E. N. (2016). Structural characteristics of pectic polysaccharides and arabinogalactan proteins from *Heracleum sosnowskyi* Manden. *Carbohydrate Polymers*, *136*, 1358–1369.

Shimizu, N., & Tomoda, M. (1985). Carbon-13 nuclear magnetic resonance spectra of alditol-form oligosaccharides having the fundamental structural units of the Malvaceae plant mucilages and a related polysaccharide. *Chemical and Pharmaceutical Bulletin*, *33*(12), 5539–5542.

Simson, B. W., & Timell, T. E. (1978). Polysaccharides in cambial tissues of *Populus tremuloides* and *Tilia americana*. IV 4-O-methylglucuronoxylan and pectin. *Cellulose Chemistry and Technology*, *12*, 79–84.

Sommer, C., Pedersen, J. S., & Stein, P. C. (2004). Apparent specific volume measurements of poly(ethylene oxide), poly(butylene oxide), poly(propylene oxide), and octadecyl chains in the micellar state as a function of temperature. *The Journal of Physical Chemistry B*, *108*(20), 6242–6249.

Šutovská, M., Capek, P., Fraňová, S., Pawlaczyk, I., & Gancarz, R. (2012). Antitussive and bronchodilatory effects of *Lythrum salicaria* polysaccharide-polyphenolic conjugate. *International Journal of Biological Macromolecules*, *51*, 794–799.

Tomoda, M., & Satoh, N. (1977). Plant mucilages XVII. Partial hydrolysis and a possible structure of paniculatan. *Chemical and Pharmaceutical Bulletin*, *25*(11), 2910–2916.

Van Holst, G.-J., & Clarke, A. E. (1985). Quantification of arabinogalactan-protein in plant extracts by single radial gel diffusion. *Analytical Biochemistry*, *148*(2), 446–450.

Vasicek, O., Lojek, A., Jancinova, V., Nosal, R., & Ciz, M. (2014). Role of histamine receptors in the effects of histamine on the production of reactive oxygen species by whole blood phagocytes. *Life Sciences*, *100*, 67–72.

Viola, H., Wolfman, C., Levi de Stein, M., Wasowski, C., Peña, C., Medina, J. H., et al. (1994). Isolation of pharmacologically active benzodiazepine receptor ligands from *Tilia tomentosa*. *Journal of Ethnopharmacology*, *44*(1), 47–53.

WHO. (2010). Flos Tiliae. In A. Zakaryan, & A. Arbor (Eds.), *WHO monographs on medicinal plants commonly used in the Newly Independent States* (pp. 393–406). Geneva: WHO Press.

Wangensteen, H., Diallo, D., & Paulsen, B. S. (2015). Medicinal plants from Mali: Chemistry and biology. *Journal of Ethnopharmacology*, *176*, 429–437.

Xie, Y., Zhang, B., & Zhang, Y. (2015). Protective effects of *Acanthopanax polysaccharides* on cerebral ischemia-reperfusion injury and its mechanisms. *International Journal of Biological Macromolecules*, *72*, 946–950.

Yakovlev, A. I. (1985). Polysaccharides of the inflorescences of *Tilia cordata*. *Chemistry of Natural Compounds*, *21*(1), 114–115.

Yamada, H., & Kiyohara, H. (2007). Immunomodulating activity of plant polysaccharide structures. In J. P. Kamerling (Ed.), *Comprehensive glycoscience – from chemistry to systems biology* (pp. 663–694). Oxford: Elsevier.

Yang, J. W., Yoon, S. Y., Oh, S. J., Kim, S. K., & Kang, K. W. (2006). Bifunctional effects of fucoidan on the expression of inducible nitric oxide synthase. *Biochemical and Biophysical Research Communications*, *346*(1), 345–350.

York, W. S., Darvill, A. G., McNeil, M., & Albersheim, P. (1985). 3-deoxy-D-manno-2-octulosonic acid (KDO) is a component of rhamnogalacturonan II, a pectic polysaccharide in the primary cell walls of plants. *Carbohydrate Research*, *138*(1), 109–126.

Zhu, Q., Liao, C., Liu, Y., Wang, P., Guo, W., He, M., et al. (2012). Ethanolic extract and water-soluble polysaccharide from *Chaenomeles speciosa* fruit modulate lipopolysaccharide-induced nitric oxide production in RAW 264.7 macrophage cells. *Journal of Ethnopharmacology*, *144*, 441–447.